

Fermi surface fluctuations and single electron excitations near Pomeranchuk instability in two dimensions

Luca Dell'Anna and Walter Metzner

Max-Planck-Institut für Festkörperforschung, D-70569 Stuttgart, Germany

(Dated: October 6, 2018)

A metallic electron system near an orientational symmetry breaking Pomeranchuk instability is characterized by a "soft" Fermi surface with enhanced collective fluctuations. We analyze fluctuation effects in a two-dimensional electron system on a square lattice in the vicinity of a Pomeranchuk instability with d-wave symmetry, using a phenomenological model which includes interactions with a small momentum transfer only. We compute the dynamical density correlations with a d-wave form factor for small momenta and frequencies, the dynamical effective interaction due to fluctuation exchange, and the electron self-energy. At the quantum critical point the density correlations and the dynamical forward scattering interaction diverge with a dynamical exponent $z = 3$. The singular forward scattering leads to large self-energy corrections, which destroy Fermi liquid behavior over the whole Fermi surface except near the Brillouin zone diagonal. The decay rate of single-particle excitations, which is related to the width of the peaks in the spectral function, exceeds the excitation energy in the low-energy limit. The dispersion of maxima in the spectra flattens strongly near those portions of the Fermi surface which are remote from the zone diagonal.

PACS: 71.10.Fd, 71.18.+y, 74.20.Mn

I. INTRODUCTION

Under suitable circumstances electron-electron interactions can generate a spontaneous breaking of the rotation symmetry of an itinerant electron system without breaking translation invariance. From a Fermi liquid perspective such an instability is driven by forward scattering interactions and leads to a symmetry breaking deformation of the Fermi surface. Alluding to a stability limit for forward scattering derived long ago by Pomeranchuk,¹ it is therefore frequently referred to as "*Pomeranchuk instability*". On a square lattice, a Pomeranchuk instability with $d_{x^2-y^2}$ symmetry, where the Fermi surface expands along the k_x axis and shrinks along the k_y axis (or vice versa), was first considered for the t-J,² Hubbard,^{3,4} and extended Hubbard model.⁵ Fermi surface symmetry breaking in fully isotropic (not lattice) systems has also been analyzed.⁶ A Pomeranchuk instability leads to a state with the same symmetry reduction as the "nematic" electron liquid defined by Kivelson et al.⁷ in their discussion of similarities between doped Mott insulators with

charge stripe correlations and liquid crystal phases.

A Pomeranchuk instability usually has to compete with other instabilities, but can also coexist with other symmetry breaking order. For example, in the two dimensional Hubbard model with a sizable next-to-nearest neighbor hopping and an electron density near van Hove filling a superconducting state with a d-wave deformed Fermi surface is stabilized at least at weak coupling.⁸ Superconducting nematic states have also been included in a general classification of possible symmetry breaking patterns by Vojta et al.⁹ In this work we will however focus on symmetry breaking Fermi surface deformations in an otherwise normal state. Since a Pomeranchuk instability of electrons on a lattice breaks only a discrete symmetry, no Goldstone mode exists and symmetry-broken states are stable also at finite temperature in $d \geq 2$ dimensions.

Electron systems in the vicinity of a Pomeranchuk instability have peculiar properties due to a "soft" Fermi surface, which can be easily deformed by anisotropic perturbations. In particular, it was shown that dynamical fluctuations of such a soft Fermi surface lead to a strongly enhanced decay rate for single-particle excitations and thus to non-Fermi liquid behavior.¹⁰ Close to a $d_{x^2-y^2}$ Pomeranchuk instability the decay rate is maximal near the k_x and k_y axes and minimal near the diagonal of the Brillouin zone. The decay rate was computed in random phase approximation (RPA) for a phenomenological model describing electrons on a square lattice which interact exclusively via scattering processes with small momentum transfers.¹⁰ Subsequently it was shown that the putative continuous Pomeranchuk transition in this model is usually preempted by a first order transition at low temperatures, that is the Fermi surface symmetry changes abruptly before the fluctuations become truly critical.^{11,12} However, for reasonable choices of hopping and interaction parameters the system is nevertheless characterized by a drastically softened Fermi surface on the symmetric side of the first order transition, and hence by strongly enhanced Fermi surface fluctuations.¹³ Furthermore, adding a uniform repulsion to the forward scattering interaction, the first order transition can be suppressed, and for a favorable but not unphysical choice of model parameters even a genuine quantum critical point can be realized.¹³

In this work we present a detailed analysis of dynamical Fermi surface fluctuations in the vicinity of a Pomeranchuk instability with $d_{x^2-y^2}$ -wave symmetry in two dimensions and their effect on single electron excitations. We compute the dynamical density correlations with a d-wave form factor for small momenta and frequencies, the dynamical effective interaction due to fluctuation exchange, and the electron self-energy, from which the spectral function for single-particle excitations is obtained. In the quantum critical regime the density correlations and the dynamical forward scattering interaction diverge with a singularity familiar from other quantum phase transitions in itinerant electron systems with dynamical exponent $z = 3$. The singular forward scattering leads to large self-energy contributions $\Sigma(\mathbf{k}, \omega)$, which are proportional to $d_{\mathbf{k}}^2$, where $d_{\mathbf{k}}$ is a form factor with d-wave

symmetry. At the quantum critical point, $\text{Im}\Sigma(\mathbf{k}_F, \omega)$ scales to zero as $|\omega|^{2/3}$. Fermi liquid behavior is thus destroyed over the whole Fermi surface except near the Brillouin zone diagonal. We also compute the crossover from non-Fermi to Fermi liquid behavior in case of a large finite correlation length ξ in the ground state. In the quantum critical regime at low finite temperatures the self-energy has a part due to quantum fluctuations, which obeys (ω/T) -scaling, but also a classical part, which is proportional to $T\xi(T)$ near the Fermi surface. The classical contribution violates (ω/T) -scaling and was overlooked in Ref. 10.

The article is structured as follows. In Sec. II we define our phenomenological model and review its mean-field phase diagram. In Sec. III we analyze the dynamical effective interaction of the model in a regime where the nearby Pomeranchuk instability leads to strong Fermi surface fluctuations. The low energy behavior of the self-energy in the presence of these fluctuations is then computed in Sec. IV, and results for the corresponding spectral function are discussed in Sec. V. We finally summarize and discuss the possible role of d-wave Fermi surface fluctuations in cuprate superconductors in Sec. VI.

II. F-MODEL

To analyze fluctuation effects in the vicinity of a Pomeranchuk instability we consider a phenomenological lattice model with an interaction which drives a Fermi surface symmetry breaking, but no other instability. The model Hamiltonian, which has been introduced already in Ref. 10, reads

$$H = \sum_{\mathbf{k}, \sigma} \epsilon_{\mathbf{k}} n_{\mathbf{k}\sigma} + \frac{1}{2V} \sum_{\mathbf{k}, \mathbf{k}', \mathbf{q}} f_{\mathbf{k}\mathbf{k}'}(\mathbf{q}) n_{\mathbf{k}}(\mathbf{q}) n_{\mathbf{k}'}(-\mathbf{q}), \quad (1)$$

where $\epsilon_{\mathbf{k}}$ is a single-particle dispersion, $n_{\mathbf{k}}(\mathbf{q}) = \sum_{\sigma} c_{\mathbf{k}-\mathbf{q}/2, \sigma}^{\dagger} c_{\mathbf{k}+\mathbf{q}/2, \sigma}$, and V is the volume of the system. Since the Pomeranchuk instability is driven by interactions with vanishing momentum transfers, that is forward scattering, we choose a function $f_{\mathbf{k}\mathbf{k}'}(\mathbf{q})$ which contributes only for relatively small momenta \mathbf{q} , and refer to the above model as the "*f-model*". Clearly this model is adequate only if the Pomeranchuk instability dominates over other instabilities and fluctuations in the system. Otherwise it would have to be supplemented by interactions with large momentum transfers.

For hopping amplitudes t , t' , and t'' between nearest, next-nearest, and third-nearest neighbors on a square lattice, respectively, the dispersion relation is given by

$$\epsilon_{\mathbf{k}} = -2 [t(\cos k_x + \cos k_y) + 2t' \cos k_x \cos k_y + t''(\cos 2k_x + \cos 2k_y)]. \quad (2)$$

For a simplified treatment, which however fully captures the crucial physics, we consider an interaction of the form

$$f_{\mathbf{k}\mathbf{k}'}(\mathbf{q}) = u(\mathbf{q}) + g(\mathbf{q}) d_{\mathbf{k}} d_{\mathbf{k}'} \quad (3)$$

with $u(\mathbf{q}) \geq 0$ and $g(\mathbf{q}) < 0$, and a form factor $d_{\mathbf{k}}$ with $d_{x^2-y^2}$ symmetry, such as $d_{\mathbf{k}} = \cos k_x - \cos k_y$. The coupling functions $u(\mathbf{q})$ and $g(\mathbf{q})$ vanish if $|\mathbf{q}|$ exceeds a certain small momentum cutoff Λ . This ansatz mimics the effective interaction in the forward scattering channel as obtained from renormalization group calculations³ and perturbation theory¹⁴ for the two-dimensional Hubbard model near van Hove filling. The uniform term originates directly from the repulsion between electrons and suppresses the electronic compressibility of the system. The d-wave term drives the Pomeranchuk instability.

The mean-field solution of the f-model has been analyzed for various choices of parameters in a series of recent articles.^{11,12,13} In the plane spanned by the chemical potential μ and temperature T the symmetry-broken phase is formed below a dome-shaped transition line $T_c(\mu)$ with a maximal transition temperature near van Hove filling. The phase transition is usually first order near the edges of the transition line, that is where T_c is relatively low, and always second order near its center.¹² The two tricritical points at the ends of the second order transition line can be shifted to lower temperatures by a sizable uniform repulsion u included in $f_{\mathbf{k}\mathbf{k}'}$.¹³ For a favorable choice of hopping and interaction parameters, with a finite t'' and $u > 0$, one of the first order edges is suppressed completely such that a quantum critical point is realized. Although quantum critical points are usually prevented by first order transitions at low temperatures in the f-model, the Fermi surface is nevertheless already very soft near the transition, such that fluctuations can be expected to be important.¹³

III. EFFECTIVE INTERACTION

In this section we derive and analyze the dynamical effective interaction for the f-model, which is closely related to the dynamical *d-wave density correlation* function¹⁵

$$N_d(\mathbf{q}, \nu) = -i \int_0^\infty dt e^{i\nu t} \langle [n_d(\mathbf{q}, t), n_d(-\mathbf{q}, 0)] \rangle, \quad (4)$$

where the d-wave density fluctuation operator is defined as

$$n_d(\mathbf{q}) = \sum_{\mathbf{k}} d_{\mathbf{k}} n_{\mathbf{k}}(\mathbf{q}). \quad (5)$$

and $n_d(\mathbf{q}, t)$ is the corresponding dynamical operator in the Heisenberg picture. We first analyze $N_d(\mathbf{q}, \nu)$ and the effective interaction within RPA, and then discuss higher order corrections.

The RPA result for the d-wave density correlation function in the f-model is simply

$$N_d(\mathbf{q}, \nu) = \frac{\Pi_d^0(\mathbf{q}, \nu)}{1 - g(\mathbf{q}) \Pi_d^0(\mathbf{q}, \nu)} \quad (6)$$

with the bare d-wave polarization function

$$\Pi_d^0(\mathbf{q}, \nu) = - \int \frac{d^2p}{(2\pi)^2} \frac{f(\epsilon_{\mathbf{p}+\mathbf{q}/2} - \mu) - f(\epsilon_{\mathbf{p}-\mathbf{q}/2} - \mu)}{\nu + i0^+ - (\epsilon_{\mathbf{p}+\mathbf{q}/2} - \epsilon_{\mathbf{p}-\mathbf{q}/2})} d_{\mathbf{p}}^2. \quad (7)$$

The infinitesimal imaginary part in the denominator specifies that we consider retarded functions. Note that the coupling $u(\mathbf{q})$ does not enter here because mixed polarization functions with a constant and a d-wave vertex vanish for small \mathbf{q} .

The RPA effective interaction is defined by the series of chain diagrams sketched in Fig. 1, yielding

$$\Gamma_{\mathbf{k}\mathbf{k}'}(\mathbf{q}, \nu) = \frac{u(\mathbf{q})}{1 - u(\mathbf{q}) \Pi^0(\mathbf{q}, \nu)} + \frac{g(\mathbf{q})}{1 - g(\mathbf{q}) \Pi_d^0(\mathbf{q}, \nu)} d_{\mathbf{k}} d_{\mathbf{k}'}, \quad (8)$$

where $\Pi^0(\mathbf{q}, \nu)$ is the conventional polarization function, defined as $\Pi_d^0(\mathbf{q}, \nu)$ but without the form factor $d_{\mathbf{k}}$.

Near the Pomeranchuk instability the denominator $1 - g(\mathbf{q}) \Pi_d^0(\mathbf{q}, \nu)$ in Eqs. (6) and (8) becomes very small for $\mathbf{q} \rightarrow \mathbf{0}$ and $\nu \rightarrow 0$, if ν vanishes faster than \mathbf{q} , while $1 - u(\mathbf{q}) \Pi^0(\mathbf{q}, \nu)$ remains of order one or even larger. The effective interaction is then dominated by the second term in Eq. (8) and can be written as

$$\Gamma_{\mathbf{k}\mathbf{k}'}(\mathbf{q}, \nu) = g S_d(\mathbf{q}, \nu) d_{\mathbf{k}} d_{\mathbf{k}'} \quad (9)$$

with $g = g(\mathbf{0})$ and the "dynamical Stoner factor"

$$S_d(\mathbf{q}, \nu) = \frac{1}{1 - g(\mathbf{q}) \Pi_d^0(\mathbf{q}, \nu)}. \quad (10)$$

The d-wave density correlation function $N_d(\mathbf{q}, \nu)$ is also proportional to $S_d(\mathbf{q}, \nu)$. In case of a second order transition the static Stoner factor

$$S_d = \lim_{\mathbf{q} \rightarrow \mathbf{0}} \lim_{\nu \rightarrow 0} S_d(\mathbf{q}, \nu) \quad (11)$$

diverges on the transition line. Near the first order transition obtained typically for low temperatures in the mean-field solution of the f-model, S_d is still drastically enhanced, that is of order ten and more.¹³

Within RPA, the dynamical d-wave density fluctuations near the Pomeranchuk instability and the corresponding singularity of the effective interaction are obviously determined by the asymptotic behavior of the d-wave polarization function $\Pi_d^0(\mathbf{q}, \nu)$ for small \mathbf{q} and ν , which we describe in the following; for derivations, see Appendix A. Analogous formulae for the expansion of the conventional polarization function $\Pi^0(\mathbf{q}, \nu)$ in three dimensions have been derived already long ago in the context of almost ferromagnetic metals by Moriya.¹⁶

At zero frequency Π_d^0 is a real function of \mathbf{q} , which can be expanded as

$$\Pi_d^0(\mathbf{q}, 0) = a(T) + c(T) |\mathbf{q}|^2 + \mathcal{O}(|\mathbf{q}|^4) \quad (12)$$

for small \mathbf{q} . The coefficient $a(T)$ is always negative and can be written as

$$a(T) = \int d\epsilon f'(\epsilon - \mu) N_{d^2}(\epsilon) \quad (13)$$

with a weighted density of states $N_{d^2}(\epsilon) = \int \frac{d^2p}{(2\pi)^2} \delta(\epsilon - \epsilon_{\mathbf{p}}) d_{\mathbf{p}}^2$. A low temperature (Sommerfeld) expansion yields

$$a(T) = -N_{d^2}(\mu) - \frac{\pi^2}{6} N_{d^2}''(\mu) T^2 + \mathcal{O}(T^4), \quad (14)$$

provided that $N_{d^2}(\mu)$ and its second derivative are finite. The coefficient $c(T)$ can be expressed as

$$c(T) = \int d\epsilon f'(\epsilon - \mu) \left[\frac{1}{48} N_{d^2v^2}''(\epsilon) - \frac{1}{16} N_{d^2\Delta\epsilon}'(\epsilon) \right], \quad (15)$$

where $N_{d^2\Delta\epsilon}(\epsilon) = \int \frac{d^2p}{(2\pi)^2} \delta(\epsilon - \epsilon_{\mathbf{p}}) d_{\mathbf{p}}^2 \Delta\epsilon_{\mathbf{p}}$ with the Laplacian $\Delta = \partial_{p_x}^2 + \partial_{p_y}^2$, and $N_{d^2v^2}(\epsilon) = \int \frac{d^2p}{(2\pi)^2} \delta(\epsilon - \epsilon_{\mathbf{p}}) d_{\mathbf{p}}^2 v_{\mathbf{p}}^2$ with $v_{\mathbf{p}} = |\nabla\epsilon_{\mathbf{p}}|$. Primes denote derivatives with respect to ϵ . The sign of $c(T)$ depends on the dispersion and other model parameters. In the low temperature limit it will be sufficient to use

$$c = c(0) = \frac{1}{16} N_{d^2\Delta\epsilon}'(\mu) - \frac{1}{48} N_{d^2v^2}''(\mu) \quad (16)$$

For finite frequencies $\Pi_d^0(\mathbf{q}, \nu)$ is generally complex. For small \mathbf{q} and ν with $\nu/|\mathbf{q}| \rightarrow 0$ its imaginary part behaves as

$$\text{Im}\Pi_d^0(\mathbf{q}, \nu) \rightarrow -\rho(\hat{\mathbf{q}}, T) \frac{\nu}{|\mathbf{q}|}, \quad (17)$$

where $\rho(\hat{\mathbf{q}}, T) > 0$ depends only on the direction $\hat{\mathbf{q}}$ of \mathbf{q} . At low temperatures it is sufficient to use $\rho(\hat{\mathbf{q}}) = \rho(\hat{\mathbf{q}}, 0)$, which can be expressed as

$$\rho(\hat{\mathbf{q}}) = \frac{1}{4\pi} \sum_{\mathbf{k}_F^0} d_{\mathbf{k}_F^0}^2 \frac{1}{v_{\mathbf{k}_F^0}} \frac{1}{|\mathbf{t}_{\mathbf{k}_F^0} \cdot \nabla_{\mathbf{k}_F^0}(\hat{\mathbf{q}} \cdot \mathbf{v}_{\mathbf{k}_F^0})|}. \quad (18)$$

Here \mathbf{k}_F^0 are points on the Fermi surface satisfying the condition $\hat{\mathbf{q}} \cdot \mathbf{v}_{\mathbf{k}_F^0} = 0$ and $\mathbf{t}_{\mathbf{k}_F^0}$ is a tangential unit vector in \mathbf{k}_F^0 . Since the velocity $\mathbf{v}_{\mathbf{k}_F^0}$ is perpendicular to the Fermi surface in \mathbf{k}_F^0 and also perpendicular to $\hat{\mathbf{q}}$, the Fermi surface has to be parallel to $\hat{\mathbf{q}}$ in \mathbf{k}_F^0 . For convex reflection symmetric Fermi surfaces in two dimensions there are two such points for each given $\hat{\mathbf{q}}$, which are antipodal to each other.

Motivated by the RPA result, but envisaging already corrections beyond RPA, we parametrize the dynamical Stoner factor for small \mathbf{q} and ν , with $\nu/|\mathbf{q}|$ also small, as follows

$$S_d(\mathbf{q}, \nu) = \frac{1}{(\xi_0/\xi)^2 + \xi_0^2 |\mathbf{q}|^2 - i \frac{\nu}{u(\hat{\mathbf{q}})|\mathbf{q}|}}. \quad (19)$$

Within RPA, the length scales ξ_0 and ξ and the velocity u are related in a simple manner to the expansion coefficients of Π_d^0 and the coupling function $g(\mathbf{q})$. Assuming that the latter can be expanded as $g(\mathbf{q}) = g + g_2 |\mathbf{q}|^2 + \dots$ for small \mathbf{q} , we get

$$\xi_0^2 = -g c(T) - g_2 a(T), \quad (20)$$

$$(\xi_0/\xi)^2 = S_d^{-1} = 1 - g a(T), \quad (21)$$

$$u(\hat{\mathbf{q}}) = -\frac{1}{g \rho(\hat{\mathbf{q}}, T)}. \quad (22)$$

For $g < 0$ the velocity $u(\hat{\mathbf{q}})$ is always positive.¹⁷ The static Stoner factor S_d diverges at the Pomeranchuk transition, if it is continuous, and the correlation length ξ diverges accordingly as $\sqrt{S_d}$. The relation for ξ_0 makes sense only if the right hand side is positive. This is guaranteed if we restrict ourselves to systems where the Pomeranchuk transition is the leading instability. For $-g c(T) - g_2 a(T) < 0$ a charge density wave instability with a wave vector $\mathbf{q} \neq \mathbf{0}$ sets in first. The parameters ξ_0 and $u(\hat{\mathbf{q}})$ remain finite at the Pomeranchuk transition and do not vary much in its vicinity. The correlation length $\xi(\delta, T)$ near the transition depends sensitively on control parameters δ , such as the chemical potential, and on the temperature. If the transition is continuous, $\xi(\delta, T)$ diverges for $T \rightarrow T_c(\delta)$. Within RPA, $\xi(\delta, T)$ diverges as $(T - T_c)^{-1/2}$ if $T_c(\delta) > 0$, and as T^{-1} if δ is tuned to a quantum critical point δ_c .

For small \mathbf{q} and ν , with $\nu/|\mathbf{q}|$ also small, the d-wave density correlation function can be written as $N_d(\mathbf{q}, \nu) = -\kappa_d^0 S_d(\mathbf{q}, \nu)$, where $\kappa_d^0 = -\lim_{\mathbf{q} \rightarrow \mathbf{0}} \lim_{\nu \rightarrow 0} \Pi_d^0(\mathbf{q}, \nu)$ is the static d-wave compressibility.¹³ Its imaginary part is then given by

$$\text{Im} N_d(\mathbf{q}, \nu) = -\kappa_d^0 \frac{\frac{\nu}{u|\mathbf{q}|}}{\left[(\xi_0/\xi)^2 + \xi_0^2 |\mathbf{q}|^2 \right]^2 + \left(\frac{\nu}{u|\mathbf{q}|} \right)^2} \quad (23)$$

For $\xi \gg \xi_0$ and small finite \mathbf{q} this function exhibits a pronounced peak at low frequencies with a steep slope for $\nu \rightarrow 0$, in agreement with recent numerical results for $N_d(\mathbf{q}, \nu)$ obtained for the t-J model within slave boson RPA.¹⁵

We now discuss corrections due to contributions beyond RPA. The exact density correlation function $N_d(\mathbf{q}, \nu)$ can be written in the form of Eq. (6), with the full polarization function $\Pi_d(\mathbf{q}, \nu)$, which is dressed by interactions, instead of the bare one. Analogously the full effective interaction is given by Eq. (8) with dressed polarization functions $\Pi(\mathbf{q}, \nu)$ and $\Pi_d(\mathbf{q}, \nu)$. Close to a continuous phase transition two types of interaction corrections

can be distinguished, namely regular interactions which remain finite at the transition and singular effective interactions associated with large order parameter fluctuations which diverge.

Corrections to RPA and corresponding subleading corrections to Fermi liquid behavior due to regular interactions, in a generic stable Fermi liquid regime, have been analyzed thoroughly in the last few years.¹⁸ The low energy behavior of most quantities receives non-analytic corrections to Fermi liquid behavior in dimensions $d \leq 3$. For example, in two dimensions the spin susceptibility varies as $|\mathbf{q}|$ instead of $|\mathbf{q}|^2$ for small \mathbf{q} at $T = 0$. Remarkably, the charge susceptibility for small \mathbf{q} remains unaffected. In this case non-analytic contributions appearing on the level of single Feynman diagrams cancel systematically when all relevant diagrams at a certain order are summed.¹⁸ The arguments establishing the cancellation of non-analytic corrections for the charge susceptibility can be readily extended to our case of a d-wave density instead of the conventional density operator.¹⁹ The crucial point is that a perturbing field coupling to the d-wave density operator does not alter the singularities in the polarization function at $\mathbf{q} = \mathbf{0}$ and $\mathbf{q} = 2\mathbf{k}_F$. Hence, corrections due to regular interactions may shift the parameters with respect to the RPA result for $N_d(\mathbf{q}, \nu)$ and $\Gamma_{\mathbf{k}\mathbf{k}'}(\mathbf{q}, \nu)$, but they do not yield any qualitative changes. Within the f-model, one such correction appears already on mean-field level: the u -term in $f_{\mathbf{k}\mathbf{k}'}(\mathbf{q})$ generates a constant (momentum-independent) Hartree self-energy correction, which renormalizes the relation between μ and density.¹³

Near a continuous phase transition order parameter correlations are strongly renormalized with respect to the mean-field or RPA result, if the dimensionality of the system is below the upper critical dimension.²⁰ These renormalizations are most naturally treated by a renormalization group analysis of an effective field theory, where the order parameter fluctuations are represented by a bosonic field. The propagator of that field corresponds to the order parameter correlation function, that is to $N_d(\mathbf{q}, \nu)$ in our case. The singular effective interaction between electrons, which is generated by large order parameter fluctuations, is then mediated by the bosonic field. In the bosonic representation, corrections to the RPA result for the order parameter correlations are due to interactions of the Bose field. Close to a continuous Pomeranchuk transition at finite T_c these terms are relevant and lead to the classical non-Gaussian asymptotic behavior of the Ising universality class in two dimensions. In the following we focus however on the behavior in the *quantum* critical regime near the zero temperature critical point at $\delta = \delta_c$. In that regime the upper critical dimension separating Gaussian from non-Gaussian behavior is $d_c = 4 - z$, where z is the dynamical exponent.²¹ In our case of a charge instability at $\mathbf{q} = \mathbf{0}$ one has $z = 3$, in complete analogy to the ferromagnetic quantum critical point in itinerant electron systems.²¹ Hence we have $d_c = 1$, while the dimensionality of our system is two, such that Gaussian behavior is stable. However, as first pointed out by Millis,²² the irrelevant quartic interaction of the order parameter fluctuations changes the temperature

dependence of the correlation length near the quantum critical point completely compared to the RPA result. In particular, in a two-dimensional system with $z = 3$, the correlation length at δ_c behaves as²²

$$\xi(\delta_c, T) \propto \frac{1}{\sqrt{T |\log T|}} \quad (24)$$

instead of the naive T^{-1} -divergence.

In summary, the d-wave density correlations and the singular part of the effective interaction in the quantum critical regime can be parametrized by the dynamical Stoner factor $S_d(\mathbf{q}, \nu)$ as in Eq. (19), where the parameters ξ_0 and $u(\hat{\mathbf{q}})$ do not vary much, while the correlation length $\xi(\delta, T)$ depends sensitively on control parameters δ and temperature. The asymptotic behavior of $\xi(\delta, T)$ in the critical region is strongly influenced by interactions of order parameter fluctuations.

IV. SELF ENERGY

We now analyze the low energy behavior of the self-energy in the presence of strong d-wave Fermi surface fluctuations. We compute the self-energy to first order in the singular interaction $\Gamma_{\mathbf{k}\mathbf{k}'}(\mathbf{q}, \nu)$, non-selfconsistently as well as selfconsistently, and then discuss the role of vertex corrections.

A. Random phase approximation

To first order in Γ , the self-energy is given by the Fock diagram in Fig. 2. The Hartree term vanishes because the expectation value of the d-wave density operator vanishes in the symmetric phase. The Fock diagram yields

$$\Sigma(\mathbf{k}, i\omega_n) = -T \sum_{\nu_n} \int \frac{d^2q}{(2\pi)^2} \Gamma_{\mathbf{k}\mathbf{k}}(\mathbf{q}, i\nu_n) G(\mathbf{k} + \mathbf{q}, i\omega_n + i\nu_n) e^{i0^+(\omega_n + \nu_n)}, \quad (25)$$

where G is the propagator of the interacting system in a self-consistent perturbation expansion, which is replaced by the bare propagator G_0 in the non-selfconsistent version. Note that we have approximated $\Gamma_{\mathbf{k}\mathbf{k}'}$ with $\mathbf{k}' = \mathbf{k} + \mathbf{q}$ by $\Gamma_{\mathbf{k}\mathbf{k}}$, which makes almost no difference since only small \mathbf{q} contribute and the effective interaction does not vary rapidly as a function of \mathbf{k} and \mathbf{k}' . Analytic continuation to the real frequency axis yields

$$\begin{aligned} \Sigma(\mathbf{k}, \omega + i0^+) = & -\frac{1}{\pi} \int d\nu \int \frac{d^2q}{(2\pi)^2} [b(\nu) \text{Im}\Gamma_{\mathbf{k}\mathbf{k}}(\mathbf{q}, \nu + i0^+) G(\mathbf{k} + \mathbf{q}, \nu + \omega + i0^+) \\ & - f(\nu) \Gamma_{\mathbf{k}\mathbf{k}}(\mathbf{q}, \nu - \omega - i0^+) \text{Im}G(\mathbf{k} + \mathbf{q}, \nu + i0^+)] , \end{aligned} \quad (26)$$

where $b(\nu) = [e^{\beta\nu} - 1]^{-1}$ and $f(\nu) = [e^{\beta\nu} + 1]^{-1}$ are the Bose and Fermi functions, respectively. It is convenient to focus on the imaginary part of Σ , from which the real

part can be easily recovered via the Kramers-Kronig relation. Using Eq. (9) to express the effective interaction by the dynamical Stoner factor, $\text{Im}\Sigma$ can be written as

$$\text{Im}\Sigma(\mathbf{k}, \omega) = -\frac{g d_{\mathbf{k}}^2}{\pi} \int d\nu \int \frac{d^2q}{(2\pi)^2} [b(\nu) + f(\nu + \omega)] \text{Im}S_d(\mathbf{q}, \nu) \text{Im}G(\mathbf{k} + \mathbf{q}, \omega + \nu). \quad (27)$$

Here and in the following G , Σ , and S_d are retarded functions, that is the real frequency axis is approached from above. The imaginary part of S_d can be written as [see Eq. (19)]

$$\text{Im}S_d(\mathbf{q}, \nu) = \frac{u(\hat{\mathbf{q}}) |\mathbf{q}| \nu}{\nu^2 + [(\xi_0/\xi)^2 + (\xi_0 |\mathbf{q}|)^2] [u(\hat{\mathbf{q}}) |\mathbf{q}|]^2}. \quad (28)$$

In the non-selfconsistent calculation one can use $\text{Im}G_0(\mathbf{p}, \omega) = -\pi\delta(\omega - \xi_{\mathbf{p}})$, where $\xi_{\mathbf{p}} = \epsilon_{\mathbf{p}} - \mu$, to perform the ν -integral analytically, which yields

$$\text{Im}\Sigma(\mathbf{k}, \omega) = g d_{\mathbf{k}}^2 \int \frac{d^2q}{(2\pi)^2} [b(\xi_{\mathbf{k}+\mathbf{q}} - \omega) + f(\xi_{\mathbf{k}+\mathbf{q}})] \text{Im}S_d(\mathbf{q}, \xi_{\mathbf{k}+\mathbf{q}} - \omega). \quad (29)$$

Since we are interested in the renormalization of low energy excitations, with \mathbf{k} close to the Fermi surface, and since only small momentum transfers \mathbf{q} contribute to the self-energy, it is convenient to introduce a local coordinate system in momentum space, centered around the Fermi point \mathbf{k}_F which is reached from \mathbf{k} by a normal projection (see Fig. 3), such that the vector $\mathbf{k} - \mathbf{k}_F$ is perpendicular to the Fermi surface in \mathbf{k}_F . We can then parametrize \mathbf{k} by the variable $k_r = \pm|\mathbf{k} - \mathbf{k}_F|$, with a positive sign for \mathbf{k} on the exterior side of the Fermi surface, and minus inside. The momentum transfer \mathbf{q} can be parametrized by a radial variable q_r and a tangential variable q_t , as shown in Fig. 3.

The excitation energy $\xi_{\mathbf{k}+\mathbf{q}}$ appearing in the above expressions for $\text{Im}\Sigma$ can be expanded as $\xi_{\mathbf{k}+\mathbf{q}} = v_{\mathbf{k}_F} k_r + v_{\mathbf{k}_F} q_r + \frac{1}{2m_t} q_t^2$ for small \mathbf{q} and \mathbf{k} near \mathbf{k}_F . The parameter m_t is given by the second derivative of $\xi_{\mathbf{k}}$ in tangential direction, $m_t^{-1} = \partial_{k_t}^2 \xi_{\mathbf{k}}|_{\mathbf{k}=\mathbf{k}_F}$. The term of order q_t^2 has been included since some asymptotic results are dominated by contributions with $|q_t| \gg |q_r|$. It is convenient to use $q'_r = q_r + \frac{1}{2m_t v_{\mathbf{k}_F}} q_t^2$ instead of q_r as integration variable (in addition to q_t), since the excitation energy $\xi_{\mathbf{k}+\mathbf{q}} = v_{\mathbf{k}_F} (k_r + q'_r)$ is linear in that variable; the corresponding Jacobi determinant is one.

1. Ground state

At $T = 0$ the combination of Bose and Fermi functions contributing to the RPA self-energy reduces to

$$b(\nu) + f(\nu + \omega) = \begin{cases} -\Theta(-\omega < \nu < 0) & \text{for } \omega > 0 \\ \Theta(0 < \nu < -\omega) & \text{for } \omega < 0 \end{cases}, \quad (30)$$

where $\Theta(\cdot) = 1$, if the inequalities in the argument are satisfied, and $\Theta(\cdot) = 0$ otherwise. In the following we restrict to the case $\omega > 0$ in derivations for definiteness, but state final results also for $\omega < 0$.

At the quantum critical point ($T = 0$, $\xi = \infty$), the non-selfconsistent RPA self-energy Eq. (29) can be written as

$$\text{Im}\Sigma(\mathbf{k}, \omega) = g d_{\mathbf{k}_F}^2 \int_{-k_r}^{\frac{\omega}{v_{\mathbf{k}_F}} - k_r} \frac{dq'_r}{2\pi} \int \frac{dq_t}{2\pi} \frac{u(\hat{\mathbf{q}}) |\mathbf{q}| [\omega - v_{\mathbf{k}_F}(k_r + q'_r)]}{[\omega - v_{\mathbf{k}_F}(k_r + q'_r)]^2 + \xi_0^4 [u(\hat{\mathbf{q}})]^2 |\mathbf{q}|^6} \quad (31)$$

for $\omega > 0$. One may impose a cutoff on the q_t -integral, which however does not affect the asymptotic behavior for small ω .

For $\mathbf{k} = \mathbf{k}_F$, that is $k_r = 0$, the asymptotic ω -dependence of $\text{Im}\Sigma$ can be extracted by introducing dimensionless variables \tilde{q}_r and \tilde{q}_t , which are defined by $q'_r = (\omega/v_{\mathbf{k}_F}) \tilde{q}_r$ and $q_t = (\xi_0^2 u_{\mathbf{k}_F})^{-1/3} \omega^{1/3} \tilde{q}_t$, respectively, where $u_{\mathbf{k}_F} = u(\mathbf{t}_{\mathbf{k}_F})$. For small ω and $k_r = 0$ the above \mathbf{q} -integral is dominated by almost tangential \mathbf{q} -vectors, that is $|q_t| \gg |q_r|$; more precisely $|q'_r|$ scales as $|q_t|^3$, and $|q_r|$ consequently as $|q_t|^2$. Hence, we can replace $|\mathbf{q}|$ by $|q_t|$ and $u(\hat{\mathbf{q}})$ by $u_{\mathbf{k}_F}$. This yields, for $\omega \rightarrow 0$,

$$\text{Im}\Sigma(\mathbf{k}_F, \omega) \rightarrow \frac{g d_{\mathbf{k}_F}^2}{v_{\mathbf{k}_F}} \frac{u_{\mathbf{k}_F}^{1/3} \omega^{2/3}}{\xi_0^{4/3}} \int_0^1 \frac{d\tilde{q}_r}{2\pi} \int_{-\infty}^{\infty} \frac{d\tilde{q}_t}{2\pi} \frac{|\tilde{q}_t| (1 - \tilde{q}_r)}{(1 - \tilde{q}_r)^2 + \tilde{q}_t^6}. \quad (32)$$

This asymptotic result does not depend on any cutoff. The definite integral can be done analytically; the result is $(4\sqrt{3}\pi)^{-1}$. For $\omega < 0$ one obtains the same with $(-\omega)^{2/3}$. Hence we have shown that

$$\text{Im}\Sigma(\mathbf{k}_F, \omega) \rightarrow \frac{g d_{\mathbf{k}_F}^2}{4\sqrt{3}\pi v_{\mathbf{k}_F}} \frac{u_{\mathbf{k}_F}^{1/3}}{\xi_0^{4/3}} |\omega|^{2/3} \quad (33)$$

for small $|\omega|$. Note that $\nu = v_{\mathbf{k}_F} q'_r - \omega = (\tilde{q}_r - 1)\omega$ vanishes faster than $|\mathbf{q}|$ for $\omega \rightarrow 0$, which justifies our expansion of $S_d(\mathbf{q}, \nu)$ for small ratios $\nu/|\mathbf{q}|$.

Not unexpectedly, $\text{Im}\Sigma(\mathbf{k}_F, \omega)$ has the same energy dependence as for the quantum critical points near phase separation²³ and ferromagnetism²⁴ in two dimensions, and also for fermions coupled to a $U(1)$ -gauge field.^{25,26} In both cases the fluctuation propagator has the same singularity structure as our Stoner factor $S_d(\mathbf{q}, \nu)$ for $\xi = \infty$. Different is, however, the d-wave form factor making $\text{Im}\Sigma(\mathbf{k}_F, \omega)$ strongly anisotropic. It is strongest near the van Hove points, while the leading terms vanish on the diagonal of the Brillouin zone. Subleading terms and contributions from interactions with large momentum transfers generate at least conventional Fermi liquid decay rates (of order $\omega^2 \log|\omega|$) on the diagonal, but faster decay may be obtained due to higher order processes which couple different parts of the Fermi surface.

A strongly anisotropic decay rate for single-particle excitations following a power-law with exponent $2/3$ has also been found for an isotropic continuum (not lattice) version of our model.⁶ However, that result was obtained for the symmetry-broken "nematic" phase, and the large anisotropic decay rate is due to the anisotropy of the nematic state and its Goldstone modes. At the quantum critical point the decay rate of the isotropic system also obeys a power law with exponent $2/3$, but now with a constant prefactor over the whole Fermi surface.

For $\mathbf{k} \neq \mathbf{k}_F$, that is finite k_r , the asymptotic behavior of $\text{Im}\Sigma(\mathbf{k}, \omega)$, Eq. (31), is obtained by rewriting the integral with a dimensionless variable \tilde{q}_r defined by $q'_r + k_r = (\omega/v_{\mathbf{k}_F}) \tilde{q}_r$, and \tilde{q}_t defined by $q_t = (\xi_0^2 u)^{-1/3} \omega^{1/3} \tilde{q}_t$. Here we approximate $u(\hat{\mathbf{q}})$ by a constant u for simplicity. In the limit $\omega \rightarrow 0$ one can replace $|\mathbf{q}|$ by $\sqrt{\tilde{q}_t^2 + k_r^2}$. Carrying out the \tilde{q}_r -integral one then obtains (including the case $\omega < 0$)

$$\text{Im}\Sigma(\mathbf{k}, \omega) = \frac{g d_{\mathbf{k}_F}^2}{2\pi v_{\mathbf{k}_F}} \frac{u^{1/3} |\omega|^{2/3}}{\xi_0^{4/3}} \int_0^\infty \frac{d\tilde{q}_t}{2\pi} \sqrt{\tilde{q}_t^2 + \kappa^2} \log \left[1 + \frac{1}{(\tilde{q}_t^2 + \kappa^2)^3} \right], \quad (34)$$

with $\kappa = (u\xi_0^2/|\omega|)^{1/3} k_r$. Two different types of asymptotic behavior are separated by the frequency scale

$$\omega_{k_r} = u\xi_0^2 |k_r|^3. \quad (35)$$

For $|\omega| \gg \omega_{k_r}$, corresponding to $\kappa \ll 1$, one recovers the result Eq. (33), while for $|\omega| \ll \omega_{k_r}$ one can expand the integrand in κ^{-1} and obtains

$$\text{Im}\Sigma(\mathbf{k}, \omega) = \frac{g d_{\mathbf{k}_F}^2}{6\pi^2 v_{\mathbf{k}_F}} \frac{1}{u \xi_0^4 k_r^4} \omega^2. \quad (36)$$

In the latter limit momentum transfers normal to the Fermi surface dominate, and the above result can thus be easily generalized to a direction dependent $u(\hat{\mathbf{q}})$ replacing u by $u(\mathbf{n}_{\mathbf{k}_F})$. Note that for small k_r , the low frequency behavior of $\text{Im}\Sigma(\mathbf{k}, \omega)$ deviates from $|\omega|^{2/3}$ -behavior only below a very small scale of order $|k_r|^3$. The same crossover behavior has already been obtained previously for fermions coupled to a gauge field.²⁶

We now analyze the behavior of $\text{Im}\Sigma(\mathbf{k}_F, \omega)$ at $T = 0$ in the symmetric phase at some small distance from the quantum critical point, where the correlation length ξ is large, but not infinite. Of interest is in particular at which scale the $|\omega|^{2/3}$ -behavior of $\text{Im}\Sigma(\mathbf{k}_F, \omega)$ is affected by a large finite ξ . Introducing the same dimensionless variables \tilde{q}_r and \tilde{q}_t as for $\xi = \infty$, one finds that the \mathbf{q} -integral is still dominated by tangential momentum transfers for small ω , such that we can approximate $|\mathbf{q}|$ by $|q_t|$ and $u(\hat{\mathbf{q}})$ by $u_{\mathbf{k}_F}$. The \tilde{q}_r -integral can then be carried out analytically, which yields

$$\text{Im}\Sigma(\mathbf{k}_F, \omega) = \frac{g d_{\mathbf{k}_F}^2}{2\pi v_{\mathbf{k}_F}} \frac{u_{\mathbf{k}_F}^{1/3} |\omega|^{2/3}}{\xi_0^{4/3}} \int_0^\infty \frac{d\tilde{q}_t}{2\pi} \tilde{q}_t \log \left[1 + \frac{1}{\tilde{q}_t^2 (\tilde{q}_t^2 + \zeta^2)^2} \right], \quad (37)$$

where $\zeta = (u_{\mathbf{k}_F} \xi_0^2 / |\omega|)^{1/3} \xi^{-1}$. The \tilde{q}_t -integral can be done analytically, leading however to a rather lengthy expression. There are two asymptotic regimes, separated by the characteristic frequency scale

$$\omega_\xi = u_{\mathbf{k}_F} \xi_0^2 / \xi^3 = u_{\mathbf{k}_F} \xi_0^{-1} S_d^{-3/2}. \quad (38)$$

For $|\omega| \gg \omega_\xi$ one has $\zeta \ll 1$, which leads back to the result Eq. (33). For $|\omega| \ll \omega_\xi$, an expansion of the integral yields the asymptotic behavior

$$\text{Im}\Sigma(\mathbf{k}_F, \omega) = \frac{g d_{\mathbf{k}_F}^2}{6\pi^2 v_{\mathbf{k}_F}} \frac{\xi^4}{u_{\mathbf{k}_F} \xi_0^4} \omega^2 \log \frac{\omega_\xi}{|\omega|}. \quad (39)$$

Hence, below the scale ω_ξ one recovers Fermi liquid behavior. Close to the quantum critical point, that is for large ξ and S_d , the crossover from $|\omega|^{2/3}$ scaling to Fermi liquid behavior sets in only for very small frequencies, and the coefficient in front of the asymptotic $\omega^2 \log \frac{\omega_\xi}{|\omega|}$ law is anomalously large. A similar non-Fermi to Fermi liquid crossover occurs near antiferromagnetic²⁷ and ferromagnetic²⁴ quantum critical points. In Fig. 4 we show the non-selfconsistent RPA result for $\text{Im}\Sigma(\mathbf{k}_F, \omega)$ in the ground state for various choices of ξ , as obtained from a numerical integration of the finite ξ analog of Eq. (31). The choice of parameters $\xi_0 = v_{\mathbf{k}_F} = 1$ corresponds to fixing a length and energy scale. The somewhat arbitrary choice of $u_{\mathbf{k}_F}$ is not very critical due to the weak dependence of the results on $u_{\mathbf{k}_F}$.

2. Low finite temperature

At $T > 0$ the self-energy in the non-selfconsistent RPA approximation, Eq. (29), can be written as

$$\begin{aligned} \text{Im}\Sigma(\mathbf{k}, \omega) &= g d_{\mathbf{k}_F}^2 \int \frac{dq'_r}{2\pi} \int \frac{dq_t}{2\pi} \{b[v_{\mathbf{k}_F}(k_r + q'_r) - \omega] + f[v_{\mathbf{k}_F}(k_r + q'_r)]\} \\ &\times \frac{u(\hat{\mathbf{q}}) |\mathbf{q}| [v_{\mathbf{k}_F}(k_r + q'_r) - \omega]}{[v_{\mathbf{k}_F}(k_r + q'_r) - \omega]^2 + [(\xi_0/\xi)^2 + (\xi_0 |\mathbf{q}|)^2]^2 [u(\hat{\mathbf{q}}) |\mathbf{q}|]^2}. \end{aligned} \quad (40)$$

To tackle the asymptotic behavior of this integral for low T , small ω and small k_r , it is instructive to consider first the special case $k_r = \omega = 0$, that is

$$\begin{aligned} \text{Im}\Sigma(\mathbf{k}_F, 0) &= g d_{\mathbf{k}_F}^2 \int \frac{dq'_r}{2\pi} \int \frac{dq_t}{2\pi} [b(v_{\mathbf{k}_F} q'_r) + f(v_{\mathbf{k}_F} q'_r)] \\ &\times \frac{u(\hat{\mathbf{q}}) |\mathbf{q}| v_{\mathbf{k}_F} q'_r}{(v_{\mathbf{k}_F} q'_r)^2 + [(\xi_0/\xi)^2 + (\xi_0 |\mathbf{q}|)^2]^2 [u(\hat{\mathbf{q}}) |\mathbf{q}|]^2}. \end{aligned} \quad (41)$$

We introduce dimensionless variables \tilde{q}_r and \tilde{q}_t via the relations $q'_r = \xi_0^2 \tilde{q}_r / \xi^3$ and $q_t = \tilde{q}_t / \xi$, respectively. We now assume that ξ diverges faster than $T^{-1/3}$ for $T \rightarrow 0$, as is indeed the case when we approach the quantum critical point from the quantum critical region.²² Then the above integral is dominated by momenta with a small ratio $v_{\mathbf{k}_F} q'_r / T$, such that the Bose function can be expanded as $b(v_{\mathbf{k}_F} q'_r) \rightarrow T / (v_{\mathbf{k}_F} q'_r)$, and the Fermi function can be neglected. Furthermore we can exploit that the integral is dominated by momenta \mathbf{q} which are almost tangential to the Fermi surface for large ξ , since $|q'_r|$ scales as $|q_t|^3$, and hence $|q_r|$ as $|q_t|^2$. We can thus replace $|\mathbf{q}|$ by $|q_t|$ and $u(\hat{\mathbf{q}})$ by $u_{\mathbf{k}_F}$. We then obtain the simple result

$$\text{Im}\Sigma(\mathbf{k}_F, 0) \rightarrow \frac{g d_{\mathbf{k}_F}^2}{\xi_0^2} T \xi \int_{-\infty}^{\infty} \frac{d\tilde{q}_r}{2\pi} \int_{-\infty}^{\infty} \frac{d\tilde{q}_t}{2\pi} \frac{u_{\mathbf{k}_F} |\tilde{q}_t|}{(v_{\mathbf{k}_F} \tilde{q}_r)^2 + (1 + \tilde{q}_t^2)^2 (u_{\mathbf{k}_F} \tilde{q}_t)^2} = \frac{g d_{\mathbf{k}_F}^2}{4v_{\mathbf{k}_F} \xi_0^2} T \xi \quad (42)$$

for $T \rightarrow 0$. A similar contribution of order $T\xi$ has been found already earlier for almost antiferromagnetic^{27,29} and almost ferromagnetic³⁰ metals. Note that $\text{Im}\Sigma(\mathbf{k}_F, 0)$ does not obey the same power law as a function of T as $\text{Im}\Sigma(\mathbf{k}_F, \omega)$ as a function of ω at $T = 0$. The $T^{2/3}$ -law proposed in Ref. 10, which one might expect by identifying T and ω scaling, does not describe the leading asymptotic behavior at low T .

We now generalize the preceding analysis to finite ω , which shall however be sufficiently small that we can still use the expansion of the Bose function and neglect the Fermi function. To this end we set $\omega = v_{\mathbf{k}_F}x/\xi$, where x is a dimensionless scaling variable which is kept fixed in the low temperature limit. Once again we introduce dimensionless integration variables \tilde{q}_r and \tilde{q}_t , now defined by $q'_r - \omega/v_{\mathbf{k}_F} = \xi_0^2 \tilde{q}_r/\xi^3$ and $q_t = \tilde{q}_t/\xi$, respectively. For $\xi \rightarrow \infty$ we can then replace q_r in $|\mathbf{q}| = \sqrt{q_t^2 + q_r^2}$ by $\omega/v_{\mathbf{k}_F}$, which yields $|\mathbf{q}| = \tilde{q}/\xi$ with $\tilde{q} = \sqrt{\tilde{q}_t^2 + x^2}$. The Bose function can again be expanded and the Fermi function neglected for $T \rightarrow 0$, if ξ diverges faster than $T^{-1/3}$. We then obtain

$$\text{Im}\Sigma(\mathbf{k}_F, \omega) \rightarrow \frac{g d_{\mathbf{k}_F}^2}{4v_{\mathbf{k}_F} \xi_0^2} T \xi l(x) \quad (43)$$

with a dimensionless scaling function

$$l(x) = \int_{-\infty}^{\infty} \frac{d\tilde{q}_r}{2\pi} \int_{-\infty}^{\infty} \frac{d\tilde{q}_t}{2\pi} \frac{4 v_{\mathbf{k}_F} u(\hat{\mathbf{q}}) \tilde{q}}{(v_{\mathbf{k}_F} \tilde{q}_r)^2 + (1 + \tilde{q}^2)^2 [u(\hat{\mathbf{q}}) \tilde{q}]^2} \quad (44)$$

The unit vector $\hat{\mathbf{q}}$ can be parametrized by x and \tilde{q}_t , it does not depend on \tilde{q}_r . Doing the elementary \tilde{q}_r -integral, the velocities $v_{\mathbf{k}_F}$ and $u(\hat{\mathbf{q}})$ in the above expression for $l(x)$ drop out completely. Carrying out the remaining \tilde{q}_t -integral, we obtain the simple universal result

$$l(x) = \frac{1}{\sqrt{1+x^2}}. \quad (45)$$

For $\omega = 0$ one has $l(0) = 1$ and the above special result for $\text{Im}\Sigma(\mathbf{k}_F, 0)$ is recovered. For large x the scaling function decays as x^{-1} . Hence, the contribution from the Bose function singularity to $\text{Im}\Sigma(\mathbf{k}_F, \omega)$ leads to a peak with a height scaling as $T\xi(T)$ and a width of order $v_{\mathbf{k}_F}/\xi(T)$. The product of height and width is thus proportional to T . Since the contribution proportional to the Bose function to $\text{Im}\Sigma(\mathbf{k}, \omega)$, Eq. (40), depends only via the linear combination $\omega - v_{\mathbf{k}_F}k_r$ on ω and k_r , the right hand side of Eq. (43) is applicable also for $\mathbf{k} \neq \mathbf{k}_F$, where it yields the contribution from the expanded Bose term for $T \rightarrow 0$, $\omega \rightarrow v_{\mathbf{k}_F}k_r$, with fixed $x = (\omega/v_{\mathbf{k}_F} - k_r)\xi$.

The above asymptotic result is entirely due to "classical" fluctuations, corresponding to the contribution with $\nu_n = 0$ to the Matsubara frequency sum in Eq. (25). The analytic continuation of that contribution to real frequencies reads

$$\Sigma^c(\mathbf{k}, \omega) = -T \int \frac{d^2q}{(2\pi)^2} \Gamma_{\mathbf{k}\mathbf{k}}(\mathbf{q}, 0) G(\mathbf{k} + \mathbf{q}, \omega) \quad (46)$$

Note that $\Gamma_{\mathbf{k}\mathbf{k}}(\mathbf{q}, 0)$ is real and does not depend on the parameter $u(\hat{\mathbf{q}})$. For $G = G_0$ one can easily show that indeed

$$\text{Im}\Sigma^c(\mathbf{k}, \omega) \rightarrow \frac{g d_{\mathbf{k}_F}^2}{4v_{\mathbf{k}_F} \xi_0^2} T \xi l[(\omega/v_{\mathbf{k}_F} - k_r)\xi] \quad (47)$$

with $l(x)$ from Eq. (45). A similar scaling behavior of the self-energy in almost antiferromagnetic metals has been derived in Ref. 29.

We now split the total self-energy as $\Sigma = \Sigma^c + \Sigma^q$, where the "quantum" contribution is obtained by summing Matsubara frequencies $\nu_n \neq 0$ in Eq. (25). After analytical continuation to real frequencies, $\text{Im}\Sigma^c$ was obtained from the Bose function singularity T/ν . To analyze $\text{Im}\Sigma^q$ for real frequencies we thus subtract T/ν from the Bose function, that is we replace $b(\nu)$ by the regular function $\bar{b}(\nu) = b(\nu) - T/\nu$ in Eq. (40). The asymptotic behavior of $\text{Im}\Sigma^q$ at low energy scales (low frequency and temperature) can be extracted by using the same dimensionless variables \tilde{q}_t and \tilde{q}_r as already in the case $T = 0$, and scaling ω as T by keeping $\tilde{\omega} = \omega/T$ fixed in the limit $T \rightarrow 0$, $\omega \rightarrow 0$. Asymptotically one can replace $|\mathbf{q}|$ by $|q_t|$ and $u(\hat{\mathbf{q}})$ by $u_{\mathbf{k}_F}$ as for $T = 0$. Furthermore one can neglect ξ^{-2} in the denominator of $\text{Im}S_d$ since ξ^{-2} scales to zero faster than $|\mathbf{q}|^2$. The \tilde{q}_t -integral can then be carried out analytically, and we obtain

$$\text{Im}\Sigma^q(\mathbf{k}_F, \omega) \rightarrow \frac{g d_{\mathbf{k}_F}^2}{v_{\mathbf{k}_F}} \frac{u_{\mathbf{k}_F}^{1/3} |\omega|^{2/3}}{\xi_0^{4/3}} s(\tilde{\omega}), \quad (48)$$

with the universal dimensionless scaling function

$$s(\tilde{\omega}) = \frac{\text{sgn}(\tilde{\omega})}{3\sqrt{3}} \int_{-\infty}^{\infty} \frac{d\tilde{q}_r}{2\pi} \left[\frac{1}{e^{\tilde{\omega}(\tilde{q}_r-1)} - 1} - \frac{1}{\tilde{\omega}(\tilde{q}_r-1)} + \frac{1}{e^{\tilde{\omega}\tilde{q}_r} + 1} \right] \frac{\tilde{q}_r - 1}{|1 - \tilde{q}_r|^{4/3}}. \quad (49)$$

Note that the above integral converges since the Bose function pole has been subtracted. A plot of $s(\tilde{\omega})$ is shown in Fig. 5. For $|\tilde{\omega}| \rightarrow \infty$ the scaling function tends to $\frac{1}{4\sqrt{3}\pi}$, and one recovers the zero temperature result, Eq. (33). The convergence to the zero temperature limit is however rather slow. For small $|\tilde{\omega}|$, $s(\tilde{\omega})$ is negative and proportional to $|\tilde{\omega}|^{-2/3}$, such that

$$\text{Im}\Sigma^q(\mathbf{k}_F, 0) \rightarrow \alpha \frac{g d_{\mathbf{k}_F}^2}{v_{\mathbf{k}_F}} \frac{u_{\mathbf{k}_F}^{1/3}}{\xi_0^{4/3}} T^{2/3}, \quad (50)$$

where $\alpha \approx -0.15$ is a numerical constant. Note that $\text{Im}\Sigma^q(\mathbf{k}_F, 0)$ is positive but smaller than the absolute value of the classical contribution for low T , since the latter is proportional to $T\xi$, such that the imaginary part of $\Sigma^c + \Sigma^q$ remains negative, as it should. For $\mathbf{k} \neq \mathbf{k}_F$, that is for finite k_r , the momentum dependence of $\text{Im}\Sigma^q(\mathbf{k}, \omega)$ is negligible for $|\omega| \gg \omega_{k_r}$, with $\omega_{k_r} = u\xi_0^2|k_r|^3$, as in the zero temperature case.

To summarize, at low finite T the RPA self-energy is given by a classical contribution Σ^c of order $T\xi$, see Eq. (47), and a quantum contribution Σ^q of order $T^{2/3}$ and $|\omega|^{2/3}$,

which obeys ω/T -scaling. For $|\omega| \gg \omega_{k_r}$ the latter is described by Eq. (48). A similar structure of the self-energy, with a classical part and a quantum part obeying (ω/T) -scaling, has been obtained already earlier for electrons coupled to strong ferromagnetic³⁰ or antiferromagnetic²⁷ fluctuations in the quantum critical regime. In the latter case the self-energy is singular at special hot spots on the Fermi surface, and Σ^q scales with an exponent $1/2$ instead of $2/3$. In Fig. 6 we show results for $\text{Im}\Sigma(\mathbf{k}_F, \omega)$ as obtained from a numerical integration of Eq. (40) at various temperatures. The correlation length has been chosen as $\xi(T) \propto (T|\log T|)^{-1/2}$, that is the temperature dependence derived by Millis.²² Analogous results for $\mathbf{k} \neq \mathbf{k}_F$ are plotted in Fig. 7. In agreement with the above asymptotic analysis the graphs show a dispersing finite T structure sitting on top of an almost momentum independent background which is proportional to $|\omega|^{2/3}$ for $T \ll |\omega|$.

B. Self-consistency

The self-energy obtained above modifies the propagator G strongly at low energy scales. We now check the self-consistency of the results obtained in the preceding subsection, that is we analyze to what extent the self-energy obtained from the self-consistent RPA, Eq. (25) with a dressed propagator G , differs from the one computed with G_0 .

1. Ground state

At $T = 0$ and for $\omega > 0$, $\text{Im}\Sigma(\mathbf{k}, \omega)$ in self-consistent RPA, Eq. (27), can be written as

$$\text{Im}\Sigma(\mathbf{k}, \omega) = -\frac{g d_{\mathbf{k}}^2}{\pi} \int_0^\omega d\epsilon \int \frac{dq'_r}{2\pi} \int \frac{dq_t}{2\pi} \text{Im}S_d(\mathbf{q}, \epsilon - \omega) \text{Im}G(\mathbf{k} + \mathbf{q}, \epsilon). \quad (51)$$

We focus on the quantum critical point, $\xi = \infty$, such that

$$\text{Im}S_d(\mathbf{q}, \nu) = \frac{u(\hat{\mathbf{q}}) |\mathbf{q}| \nu}{\nu^2 + \xi_0^4 [u(\hat{\mathbf{q}})]^2 |\mathbf{q}|^6}. \quad (52)$$

Motivated by the perturbative results in Sec. IV.A, we assume that the low-frequency behavior of $\text{Im}\Sigma(\mathbf{k}_F, \omega)$ is given by $C_2 |\omega|^{2/3}$, where C_2 is a negative constant, and $\text{Im}\Sigma(\mathbf{k}, \omega)$ with a small distance k_r from the Fermi surface is given by the same behavior for frequencies above the small scale $\omega_{k_r} = u\xi_0^2 k_r^3$. The analytical properties of Σ in the complex plane then dictate

$$\text{Re}\Sigma(\mathbf{k}_F, \omega) = -\frac{\omega}{\pi} \mathcal{P} \int_{-\infty}^{\infty} d\omega' \frac{C_2 |\omega'|^{2/3}}{(\omega - \omega') \omega'} = C_1 \text{sgn}(\omega) |\omega|^{2/3}, \quad (53)$$

where \mathcal{P} denotes the principal value and $C_1 = \sqrt{3} C_2$. Anticipating that for small ω and $\mathbf{k} = \mathbf{k}_F$ the integral in Eq. (51) is dominated by contributions with $\epsilon \gg u\xi_0^2 q_r^3$, we can

approximate

$$\text{Im}G(\mathbf{k}_F + \mathbf{q}, \epsilon) = \frac{C_2 |\epsilon|^{2/3}}{[\epsilon - v_{\mathbf{k}_F} q'_r - C_1 \text{sgn}(\epsilon) |\epsilon|^{2/3}]^2 + (C_2 |\epsilon|^{2/3})^2} \quad (54)$$

under the integral. Scaling out the ω -dependence from the integral in Eq. (51) one finds that the integration variable ϵ scales as ω , q_t as $\omega^{1/3}$, and q'_r as $\omega^{2/3}$. Hence, for small ω one can replace $|\mathbf{q}|$ by $|q_t|$ and $u(\hat{\mathbf{q}})$ by $u_{\mathbf{k}_F}$. This implies that the q'_r -integration acts only on $\text{Im}G$, yielding simply

$$\int \frac{dq'_r}{2\pi} \text{Im}G(\mathbf{k}_F + \mathbf{q}, \epsilon) = -\frac{1}{2v_{\mathbf{k}_F}}. \quad (55)$$

This is independent of C_1 and C_2 , which means that the self-energy drops out completely! Carrying out the integral over ϵ and q_t one then recovers the result for $\text{Im}\Sigma(\mathbf{k}_F, \omega)$ obtained already within the non-selfconsistent RPA. Hence, the replacement of G_0 by G does not affect the asymptotic low frequency behavior of $\text{Im}\Sigma(\mathbf{k}_F, \omega)$ at all, it does not even modify the prefactor. The same result has already been obtained earlier in the formally similar problem of fermions coupled to a $U(1)$ -gauge field,²⁸ and also for antiferromagnetic quantum critical points.²⁷

The above arguments can be easily extended to the case $\mathbf{k} \neq \mathbf{k}_F$ with a small finite k_r , since the latter affects $\text{Im}\Sigma(\mathbf{k}, \omega)$ only for frequencies below the small scale $\omega_{k_r} \propto k_r^3$.

2. Low finite temperature

We first analyze to what extent the peak-shaped classical contribution to $\text{Im}\Sigma(\mathbf{k}, \omega)$ is modified by self-energy feedback into G . As before, we compute this contribution by expanding the Bose function, $b(\nu) \approx T/\nu$, which yields

$$\text{Im}\Sigma^c(\mathbf{k}, \omega) = -\frac{g d_{\mathbf{k}}^2}{\pi} T \int \frac{d\nu}{\nu} \int \frac{dq'_r}{2\pi} \int \frac{dq_t}{2\pi} \text{Im}S_d(\mathbf{q}, \nu) \text{Im}G(\mathbf{k} + \mathbf{q}, \omega + \nu), \quad (56)$$

where G is the full propagator. To scale out ξ from $\text{Im}S_d(\mathbf{q}, \nu)$, we use dimensionless variables $\tilde{\nu}$ and \tilde{q} defined by $\nu = v_{\mathbf{k}_F} \xi_0^2 \tilde{\nu}/\xi^3$ and $|\mathbf{q}| = \tilde{q}/\xi$, respectively, such that

$$\text{Im}S_d(\mathbf{q}, \nu) = \frac{\xi^2}{\xi_0^2} \frac{v_{\mathbf{k}_F} u(\hat{\mathbf{q}}) \tilde{q} \tilde{\nu}}{v_{\mathbf{k}_F}^2 \tilde{\nu}^2 + (1 + \tilde{q}^2)^2 [u(\hat{\mathbf{q}}) \tilde{q}]^2}. \quad (57)$$

The inverse propagator can be written as $G^{-1}(\mathbf{k} + \mathbf{q}, \omega + \nu) = \omega + \nu - v_{\mathbf{k}_F} (k_r + q'_r) - \Sigma(\mathbf{k} + \mathbf{q}, \omega + \nu)$.

Consider first the case $\mathbf{k} = \mathbf{k}_F$ and $\omega = 0$. Then $\Sigma(\mathbf{k} + \mathbf{q}, \omega + \nu)$ can be replaced by $\Sigma(\mathbf{k}_F + \mathbf{q}, 0)$ for $T \rightarrow 0$, since ν scales to zero as ξ^{-3} . Motivated by the perturbative result we assume that $\text{Im}\Sigma(\mathbf{k}, 0)$ is of order $T\xi$ for $\mathbf{k} = \mathbf{k}_F$ and decreases for momenta

away from \mathbf{k}_F . Note that $T\xi \propto (\xi \log \xi)^{-1}$, since $\xi(T) \propto (T \log T)^{-1/2}$. Then ν can be neglected completely in the expression for the propagator, such that $G^{-1}(\mathbf{k}_F + \mathbf{q}, \nu) = -v_{\mathbf{k}_F} q'_r - \Sigma_{\mathbf{k}_F}(q'_r, 0)$, where $\Sigma_{\mathbf{k}_F}(q'_r, \omega) = \Sigma(\mathbf{k}_F + \mathbf{q}, \omega)$. Now the integral over ν acts only on $\text{Im}S_d$, yielding

$$\int \frac{d\nu}{\nu} \text{Im}S_d(\mathbf{q}, \nu) = \pi \frac{\xi^2}{\xi_0^2} \frac{1}{1 + \tilde{q}^2} = \pi S_d(\mathbf{q}, 0). \quad (58)$$

Writing $\tilde{q}^2 = \tilde{q}_r^2 + \tilde{q}_t^2$, we can also carry out the integral over q_t and obtain

$$\int \frac{dq_t}{2\pi} \int \frac{d\nu}{\nu} \text{Im}S_d(\mathbf{q}, \nu) = \frac{\pi}{2} \frac{\xi}{\xi_0^2} \frac{1}{\sqrt{1 + \tilde{q}_r^2}}. \quad (59)$$

Using $q'_r \approx q_r = \tilde{q}_r/\xi$ and collecting all terms we get

$$\text{Im}\Sigma^c(\mathbf{k}_F, 0) = \frac{g d_{\mathbf{k}_F}^2}{2 \xi_0^2} T \xi \int \frac{d\tilde{q}_r}{2\pi} \frac{1}{\sqrt{1 + \tilde{q}_r^2}} \text{Im} \frac{1}{v_{\mathbf{k}_F} \tilde{q}_r + \xi \Sigma_{\mathbf{k}_F}(\tilde{q}_r/\xi, 0)}. \quad (60)$$

The perturbative result for the self-energy indicates that $\Sigma_{\mathbf{k}_F}(\tilde{q}_r/\xi, 0)$ is of order $T\xi$. For $\xi(T) \propto (T |\log T|)^{-1/2}$ the self-energy correction $\xi \Sigma_{\mathbf{k}_F}(\tilde{q}_r/\xi, 0)$ in the above integral is then suppressed as $1/\log \xi$ for $T \rightarrow 0$ ($\xi \rightarrow \infty$) and can thus be neglected compared to \tilde{q}_r , albeit only with logarithmic accuracy, such that $\text{Im}[v_{\mathbf{k}_F} \tilde{q}_r + \xi \Sigma_{\mathbf{k}_F}(\tilde{q}_r/\xi, 0)]^{-1} \rightarrow \pi v_{\mathbf{k}_F}^{-1} \delta(\tilde{q}_r)$ and we recover the perturbative result Eq. (42) for $\text{Im}\Sigma(\mathbf{k}_F, 0)$. More generally, the perturbative result is not modified (asymptotically) in a self-consistent treatment as long as $\xi(T)$ increases slower than $T^{-1/2} |\log T|^{1/2}$ for $T \rightarrow 0$.³¹

For general \mathbf{k} (at or away from \mathbf{k}_F) and finite ω we can still neglect ν in G , such that $G^{-1}(\mathbf{k} + \mathbf{q}, \omega + \nu) = \omega - v_{\mathbf{k}_F}(k_r + q'_r) - \Sigma_{\mathbf{k}_F}(k_r + q'_r, \omega)$. Then $\text{Im}S_d$ can again be integrated independently over ν and q_t , which yields

$$\text{Im}\Sigma^c(\mathbf{k}, \omega) = \frac{g d_{\mathbf{k}_F}^2}{2 \xi_0^2} T \xi \int \frac{d\tilde{q}_r}{2\pi} \frac{1}{\sqrt{1 + \tilde{q}_r^2}} \text{Im} \frac{1}{v_{\mathbf{k}_F} \tilde{q}_r + \xi [v_{\mathbf{k}_F} k_r - \omega + \Sigma_{\mathbf{k}_F}(k_r + \tilde{q}_r/\xi, \omega)]}. \quad (61)$$

The classical contribution to the self-energy feedback in the above integral is again suppressed at least as $1/\log \xi$, such that only the quantum contribution Σ^q remains on the right hand side. The latter is not negligible at $\omega \neq 0$, it rather dominates over the bare frequency dependence of G for small finite ω . Let us assume that the RPA result for Σ^q is not modified qualitatively by self-consistency, as will be indeed verified below. For $k_r = 0$ or k_r scaling to zero more rapidly than $|\omega|^{1/3}$ one thus has simply $\Sigma_{\mathbf{k}_F}(k_r + \tilde{q}_r/\xi, \omega) \rightarrow \Sigma_{\mathbf{k}_F}^q(\omega)$, where $\Sigma_{\mathbf{k}_F}^q(\omega)$ is of order $|\omega|^{2/3}$ for small ω, T with $T \ll |\omega|$ and of order $T^{2/3}$ for small ω, T with $|\omega| \ll T$. In the latter case Σ^q is smaller than Σ^c , such that the self-energy feedback can be neglected completely. For $|\omega - v_{\mathbf{k}_F} k_r| \ll |\Sigma_{\mathbf{k}_F}^q(\omega)|$, the term $\omega - v_{\mathbf{k}_F} k_r$ can be neglected in Eq. (61), such that $\text{Im}\Sigma^c(\mathbf{k}, \omega)$ becomes independent of k_r and the frequency dependence is given by a scaling function which decreases monotonically with

a dimensionless scaling variable proportional to $\xi|\omega|^{2/3}$. Hence, in the self-consistent calculation $\text{Im}\Sigma^c(\mathbf{k}, \xi_{\mathbf{k}})$ is not k_r -independent but rather decreases with increasing $|k_r|$ on a scale of order $\xi^{-3/2}$, that is quite rapidly. For $|\omega - v_{\mathbf{k}_F}k_r| \gg |\Sigma_{\mathbf{k}_F}^q(\omega)|$ the self-energy feedback is negligible and one recovers the non-selfconsistent RPA result. In general one will find a crossover between the limiting cases. In particular, the decrease of $\text{Im}\Sigma^c(\mathbf{k}_F, \omega)$ as a function of increasing $|\omega|$ occurs on a scale of order $\xi^{-3/2}$ for the smallest frequencies and then, more slowly, on the larger scale ξ^{-1} . For $\mathbf{k} \neq \mathbf{k}_F$ the self-consistent result for $\text{Im}\Sigma^c(\mathbf{k}, \omega)$ depends on k_r and ω in a more complicated way than just via the difference $\omega - v_{\mathbf{k}_F}k_r$. Asymptotically it depends only on ω if k_r scales to zero faster than $|\omega|^{2/3}$.

We now check possible modifications of Σ^q due to self-energy feedback at low finite temperatures. Subtracting the pole from the Bose function, the quantum contribution to Eq. (27) can be written as

$$\begin{aligned} \text{Im}\Sigma^q(\mathbf{k}, \omega) = & -\frac{g d_{\mathbf{k}}^2}{\pi} \int d\nu \int \frac{dq'_r}{2\pi} \int \frac{dq_t}{2\pi} \left[b(\nu) - \frac{T}{\nu} + f(\nu + \omega) \right] \\ & \times \text{Im}S_d(\mathbf{q}, \nu) \text{Im}G(\mathbf{k} + \mathbf{q}, \omega + \nu) . \end{aligned} \quad (62)$$

We consider the case $\mathbf{k} = \mathbf{k}_F$. Frequencies are scaled with temperature, that is $\omega = T\tilde{\omega}$ and $\nu = T\tilde{\nu}$. At low T and ω one can, once again, replace $|\mathbf{q}|$ by $|q_t|$ and $u(\hat{\mathbf{q}})$ by $u_{\mathbf{k}_F}$ in $\text{Im}S_d(\mathbf{q}, \nu)$, and neglect ξ^{-2} . Then the q'_r -integration acts only on $\text{Im}G$. The inverse propagator can be written as $G^{-1}(\mathbf{k}_F + \mathbf{q}, \omega + \nu) = \omega + \nu - v_{\mathbf{k}_F}q'_r - \Sigma_{\mathbf{k}_F}^c(q'_r, \omega + \nu) - \Sigma_{\mathbf{k}_F}^q(q'_r, \omega + \nu)$. The question now is whether $\Sigma_{\mathbf{k}_F}^c(q'_r, \omega + \nu)$ leads to a significant q'_r -dependence, which could spoil the simple result Eq. (55) for the q'_r -integral of $\text{Im}G$. Since $\omega + \nu$ scales to zero as T , and thus faster than $\xi^{-3/2}$, one can replace $\Sigma_{\mathbf{k}_F}^c(q'_r, \omega + \nu)$ by $\Sigma_{\mathbf{k}_F}^c(q'_r, 0)$. The latter tends to the constant $\Sigma_{\mathbf{k}_F}^c(0, 0)$ for $|q'_r| \ll \xi^{-1}$. The largest $|q'_r|$ contributing to $\int dq'_r \text{Im}G$ are proportional to $T\xi$, which indeed scales to zero faster than ξ^{-1} for $T \rightarrow 0$, albeit only by a factor of order $\log T$. Hence, to logarithmic accuracy, we can indeed neglect the q'_r -dependence of the self-energy in $\int dq'_r \text{Im}G$, such that the simple formula Eq. (55) is still valid, and the non-selfconsistent result for $\text{Im}\Sigma^q(\mathbf{k}_F, \omega)$ is confirmed. The same result is obtained by the same arguments for $\mathbf{k} \neq \mathbf{k}_F$.

A comparison of the asymptotic result for Σ^c with a numerical evaluation of the self-consistency equations reveals that the feedback of Σ^c into Eq. (61) becomes negligible only on extremely small energy scales. This is not surprising as we have shown that this feedback vanishes only logarithmically. By contrast, the effects of self-energy feedback into Σ^q are indeed relatively small also for finite temperatures and frequencies. In the following, we therefore use the non-selfconsistent RPA result for Σ^q , but compute Σ^c from

a self-consistent solution of the complex version of Eq. (61), that is

$$\begin{aligned} \Sigma^c(\mathbf{k}, \omega) &= \frac{g d_{\mathbf{k}_F}^2}{2 \xi_0^2} T \int \frac{dq_r}{2\pi} \frac{1}{\sqrt{\xi^{-2} + q_r^2}} \\ &\times \frac{1}{v_{\mathbf{k}_F}(q_r + k_r) - \omega + \Sigma_{\mathbf{k}_F}^q(k_r + q_r, \omega) + \Sigma_{\mathbf{k}_F}^c(k_r + q_r, \omega)}. \end{aligned} \quad (63)$$

This equation can be easily solved numerically by iteration. Due to the weak radial momentum dependence of Σ^q one can neglect the q_r -dependence in its argument. Instead of using the asymptotic scaling form of Σ^q , which is valid only at sufficiently low ω and T , we compute Σ^q by integrating Eq. (40) numerically and subtracting the classical contribution. In Figs. 8 and 9 we show results for $\text{Im}\Sigma(\mathbf{k}, \omega)$ as obtained by the above procedure. One can see that the self-energy feedback suppresses the peak generated by classical fluctuations, the effect being of course stronger for larger $g d_{\mathbf{k}_F}^2$.

In summary, self-energy feedback in a self-consistent calculation affects only the contribution from classical fluctuations to $\Sigma(\mathbf{k}, \omega)$ at $T > 0$.

C. Vertex corrections

At zero temperature, vertex corrections and their feedback on the self-energy have been analyzed in detail by Altshuler et al.²⁸ for fermions coupled to a $U(1)$ -gauge field, which share many features with our model. They showed that vertex corrections may lead to moderate finite renormalizations, but the qualitative behavior of the self-energy, in particular the power-law with the exponent $2/3$, remains unchanged. This was confirmed by a renormalization group analysis of the gauge theory, and also for the formally similar case of a quantum critical point near phase separation.³² The arguments used in the above works can be directly transferred to our system and will not be repeated here.

We have not performed a complete analysis of vertex corrections at finite temperatures. By virtue of ω/T -scaling, one may expect that quantum contributions (from finite Matsubara frequencies) to vertex corrections behave similarly at zero and low finite temperatures, and lead to finite renormalizations only. By contrast, contributions from classical fluctuations at $T > 0$ have no counterpart at $T = 0$ and may thus behave differently. We have therefore analyzed the first order vertex correction (see Fig. 10) due to classical fluctuations in the quantum critical regime. In the static limit, $\nu = 0$ and $\mathbf{q} \rightarrow \mathbf{0}$, the classical contribution to the first order vertex correction is given by

$$\gamma_{\mathbf{k}_F}^c(\mathbf{0}, 0) \propto T \int d^2 q' [G(\mathbf{k}_F + \mathbf{q}', 0)]^2 S_d(\mathbf{q}', 0) \quad (64)$$

Integrating $S_d(\mathbf{q}', 0)$ over q'_t and using $q'_r = \tilde{q}_r/\xi$, one obtains

$$\gamma_{\mathbf{k}_F}^c(\mathbf{0}, 0) \propto T \xi^2 \int \frac{d\tilde{q}_r}{\sqrt{1 + \tilde{q}_r^2}} \frac{1}{[v_{\mathbf{k}_F} \tilde{q}_r + \xi \Sigma_{\mathbf{k}_F}(\tilde{q}_r/\xi, 0)]^2} \quad (65)$$

For $T \rightarrow 0$, the self-energy term $\xi \Sigma_{\mathbf{k}_F}(\tilde{q}_r/\xi, 0)$ is of order $T\xi^2$ for small \tilde{q}_r , and vanishes thus logarithmically. The above integral diverges thus logarithmically as $(T\xi^2)^{-1}$, which cancels precisely the prefactor. Hence, the classical vertex correction remains finite.

We have not analyzed any higher order vertex corrections. However, by virtue of the above results and arguments we do not expect that vertex corrections modify the RPA results for the self-energy drastically in the quantum critical regime.

V. SINGLE PARTICLE EXCITATIONS

The momentum resolved spectral function for single particle excitations is given by

$$A(\mathbf{k}, \omega) = -\frac{1}{\pi} \text{Im} \frac{1}{\omega - \xi_{\mathbf{k}} - \Sigma(\mathbf{k}, \omega)} = \frac{\pi^{-1} |\text{Im}\Sigma(\mathbf{k}, \omega)|}{[\omega - \xi_{\mathbf{k}} - \text{Re}\Sigma(\mathbf{k}, \omega)]^2 + [\text{Im}\Sigma(\mathbf{k}, \omega)]^2}, \quad (66)$$

where $\xi_{\mathbf{k}} = \epsilon_{\mathbf{k}} - \mu$ and $\Sigma(\mathbf{k}, \omega)$ is the self-energy computed in the preceding section. Close to the Fermi surface the self-energy for our model obeys the symmetry relations $\text{Re}\Sigma_{\mathbf{k}_F}(-k_r, -\omega) = -\text{Re}\Sigma_{\mathbf{k}_F}(k_r, \omega)$ and $\text{Im}\Sigma_{\mathbf{k}_F}(-k_r, -\omega) = \text{Im}\Sigma_{\mathbf{k}_F}(k_r, \omega)$, which implies $A_{\mathbf{k}_F}(-k_r, -\omega) = A_{\mathbf{k}_F}(k_r, \omega)$, since $\xi_{\mathbf{k}} = v_{\mathbf{k}_F} k_r$ for small k_r .

A. Ground state

In Fig. 11 we show results for the spectral function $A(\mathbf{k}, \omega)$ as a function of ω for several choices of k_r . The underlying self-energy has been computed at the quantum critical point ($T = 0$ and $\xi = \infty$) by integrating Eq. (31) numerically. In the following we discuss the most important features by using the analytical results from Sec. IV.

At the quantum critical point the asymptotic low-energy result for the self-energy can be summarized as

$$\Sigma(\mathbf{k}, \omega) \rightarrow \Sigma_{\mathbf{k}_F}(\omega) = -C_{\mathbf{k}_F} \left[\text{sgn}(\omega) + \frac{i}{\sqrt{3}} \right] |\omega|^{2/3}, \text{ where } C_{\mathbf{k}_F} = \frac{|g| d_{\mathbf{k}_F}^2 u_{\mathbf{k}_F}^{1/3}}{4\pi v_{\mathbf{k}_F} \xi_0^{4/3}}. \quad (67)$$

Strictly speaking this simple k_r -independent behavior is valid only for $|\omega| \gg \omega_{k_r}$, but the scale ω_{k_r} is proportional to k_r^3 and thus tiny for \mathbf{k} near the Fermi surface. The prefactor $C_{\mathbf{k}_F}$ depends strongly on the position of \mathbf{k}_F . It decreases rapidly for \mathbf{k}_F near the Brillouin zone diagonal, where $d_{\mathbf{k}_F}$ vanishes, while it is enhanced near the van Hove points, where $v_{\mathbf{k}_F}$ becomes small. The \mathbf{k}_F -dependence of $u_{\mathbf{k}_F}^{1/3}$ is comparatively weak. The competition between ω and the self-energy in the denominator of $A(\mathbf{k}, \omega)$, Eq. (66), leads to the characteristic energy scale

$$\omega_c = C_{\mathbf{k}_F}^3 \propto \frac{d_{\mathbf{k}_F}^6}{v_{\mathbf{k}_F}^3}, \quad (68)$$

which obviously varies very strongly with \mathbf{k}_F .

For fixed \mathbf{k} with $|\xi_{\mathbf{k}}| \gg \omega_c$ the spectral function $A(\mathbf{k}, \omega)$ has almost Lorentzian shape as a function of ω , with a maximum near $\omega = \xi_{\mathbf{k}}$ and a width of order $C_{\mathbf{k}_F} |\xi_{\mathbf{k}}|^{2/3}$. The lifetime broadening thus decreases more slowly than the excitation energy $\xi_{\mathbf{k}}$, as \mathbf{k} approaches the Fermi surface, such that no well-defined quasi-particles exist. For $|\xi_{\mathbf{k}}| \approx \omega_c$ the maximum of $A(\mathbf{k}, \omega)$ is shifted strongly away from $\xi_{\mathbf{k}}$ and the width is of order of the peak energy. For $|\xi_{\mathbf{k}}| \ll \omega_c$ one can neglect ω compared to $\text{Re}\Sigma(\mathbf{k}, \omega)$ in Eq. (66), and $A(\mathbf{k}, \omega)$ is now peaked at $\omega = \bar{\xi}_{\mathbf{k}}$, with the renormalized energy scale

$$\bar{\xi}_{\mathbf{k}} = \text{sgn}(\xi_{\mathbf{k}}) (C_{\mathbf{k}_F}^{-1} |\xi_{\mathbf{k}}|)^{3/2} \propto k_r^{3/2}. \quad (69)$$

Extracting a dispersion relation from the momentum dependence of the peak position in $A(\mathbf{k}, \omega)$ one thus obtains a flat band with a vanishing slope near the Fermi surface. The width of the peak centered around $\bar{\xi}_{\mathbf{k}}$ is of order $C_{\mathbf{k}_F} |\bar{\xi}_{\mathbf{k}}|^{2/3} = |\xi_{\mathbf{k}}|$ and thus linear in k_r . For $\mathbf{k} = \mathbf{k}_F$ the spectral function diverges as $|\omega|^{-2/3}$ for $\omega \rightarrow 0$.

Momentum scans of $A(\mathbf{k}, \omega)$ perpendicular to the Fermi surface at fixed ω lead to Lorentzian peaks centered around $k_r = \frac{1}{v_{\mathbf{k}_F}} [\omega + C_{\mathbf{k}_F} \text{sgn}(\omega) |\omega|^{2/3}]$. Some such scans are shown in Fig. 12 for various choices of ω . The integral

$$\int \frac{dk_r}{2\pi} A(\mathbf{k}, \omega) = \frac{1}{2\pi v_{\mathbf{k}_F}} \quad (70)$$

does not depend on the self-energy. The \mathbf{k} -integrated density of states near the Fermi level remains therefore unrenormalized, that is, it is determined by the bare Fermi velocity.

B. Low finite temperature

At low finite T the results for the self-energy can be summarized as follows. The total self-energy is a sum of two distinct contributions, $\Sigma = \Sigma^c + \Sigma^q$, where Σ^c is due to classical, and Σ^q due to quantum fluctuations. The quantum contribution Σ^q can be computed from non-selfconsistent RPA and obeys (ω/T) -scaling at very low ω and T , see Eq. (48). Its dependence on k_r is very weak. The classical contribution Σ^c is affected more strongly by self-energy feedback, especially by feedback of Σ^q . We compute Σ^c by solving Eq. (63) self-consistently. The classical part violates (ω/T) -scaling and depends significantly on k_r .

The most significant temperature effect is that $\text{Im}\Sigma(\mathbf{k}_F, 0)$ increases quickly from zero to sizable finite values upon increasing T . For small T near the quantum critical point we obtained

$$\text{Im}\Sigma(\mathbf{k}_F, 0) \rightarrow \frac{g d_{\mathbf{k}_F}^2}{4v_{\mathbf{k}_F} \xi_0^2} T \xi \propto \frac{d_{\mathbf{k}_F}^2}{v_{\mathbf{k}_F}} \sqrt{\frac{T}{|\log T|}} \quad (71)$$

both in the non-selfconsistent and self-consistent calculation. This cuts off the divergence of $A(\mathbf{k}_F, \omega)$ for $\omega \rightarrow 0$ occurring at zero temperature and replaces it by a maximum of order

$\sqrt{|\log T|/T}$. Note that $\text{Im}\Sigma(\mathbf{k}_F, 0)$ vanishes much slower with T than in conventional Fermi liquids, where one has T^2 (in 3D) or $T^2|\log T|$ (in 2D) behavior.

In Fig. 13 we show results for $A(\mathbf{k}, \omega)$ as a function of ω for various choices of k_r at a fixed low temperature. The underlying self-energy has been computed by the procedure described at the end of Sec. IV.B. The most striking differences compared to the ground state results (Fig. 11) are of course seen for \mathbf{k} near \mathbf{k}_F , where the peaks are now much broader. Note also the steep shoulder near $\omega = 0$ for the spectra with \mathbf{k} near \mathbf{k}_F at strong coupling (lower panel). The complementary view, $A(\mathbf{k}, \omega)$ as a function of k_r for various fixed ω , is shown in Fig. 14. Here the line shape resembles a Lorentzian function with a relatively large width.

VI. CONCLUSION

In summary, we have presented a detailed analysis of quantum critical fluctuations and their effect on single-particle excitations in a two-dimensional electron system close to a d-wave Pomeranchuk instability. The fluctuations can be viewed as long-wavelength density fluctuations with a d-wave form factor and also as d-wave shaped fluctuations of the Fermi surface. They lead to a strong singularity in the dynamical d-wave density correlation function at small momenta and frequencies, and to singular forward scattering. The momentum and energy dependence of the singularity is captured essentially correctly by a Gaussian theory (RPA); interactions of fluctuations modify only the temperature dependence of the correlation length $\xi(T)$.

Single-particle excitations are strongly affected by the fluctuations. We have analyzed the electron self-energy $\Sigma(\mathbf{k}, \omega)$ within plain and self-consistent RPA, focussing especially on the low-energy behavior in the quantum critical regime. The dominant contributions due to singular forward scattering are proportional to $d_{\mathbf{k}}^2$, where $d_{\mathbf{k}}$ is a form factor with d-wave symmetry, such as $\cos k_x - \cos k_y$. For \mathbf{k} near the Fermi surface this leads to a strong tangential momentum dependence of $\Sigma(\mathbf{k}, \omega)$. The singular contributions vanish on the diagonal of the Brillouin zone, and have the largest amplitude near the van Hove points. By contrast, the momentum dependence of $\Sigma(\mathbf{k}, \omega)$ perpendicular to the Fermi surface is much weaker at low temperatures. Hence, momentum scans of the spectral function perpendicular to the Fermi surface have almost Lorentzian line shape.

At the quantum critical point, the real and imaginary parts of the self-energy scale as $|\omega|^{2/3}$ with energy. This leads to a complete destruction of quasi-particles near the Fermi surface except on the Brillouin zone diagonal, due to the prefactor $d_{\mathbf{k}}^2$. The dispersion of the maxima of the spectral function $A(\mathbf{k}, \omega)$ flattens strongly for momenta \mathbf{k} near the Fermi surface away from the zone diagonal. On the other hand, the momentum integrated density of states is not renormalized significantly by the Fermi surface fluctuations.

In the quantum critical regime at $T > 0$ the self-energy consists of a "classical" and a

”quantum” part with very different dependences on T and ω . The classical part, which is due to classical fluctuations, dominates at $\omega = 0$, where it yields a contribution proportional to $T\xi(T)$ to $\text{Im}\Sigma(\mathbf{k}_F, \omega)$. The quantum part is generated by quantum fluctuations and obeys (ω/T) -scaling in the quantum critical regime.

We finally discuss whether soft Fermi surfaces and critical Fermi surface fluctuations could play a role in cuprate superconductors. Due to the coupling of electron and lattice degrees of freedom a symmetry-breaking Fermi surface deformation is generally accompanied by a lattice distortion, and vice versa. Structural transitions which reduce the lattice symmetry of the cuprate-planes are quite frequent in cuprates. Close to a Pomeranchuk instability of the electronic system, electronic properties can be expected to react unusually strongly to slight lattice distortions which break the symmetry of the electronic system explicitly. Such ”overreactions” of electronic properties have indeed been observed early on in several cuprate compounds.^{33,34} In particular, a slight orthorhombicity of the lattice structure would lead to a relatively strong orthorhombic distortion of the Fermi surface. Yamase and Kohno³⁵ invoked this idea already a few years ago to explain peculiarities of magnetic excitations in cuprates. Recent experiments on YBCO have established a remarkably strong in-plane anisotropy of electronic and magnetic properties,^{36,37,38} although the structural anisotropy of the CuO_2 -planes, which is induced indirectly by the CuO -chains between the planes in that material, is relatively modest.³⁹ Fermi surface softening with d-wave symmetry due to forward scattering interactions can naturally amplify the effect of a weak or moderate structural anisotropy.

Since the Pomeranchuk instability breaks the orientational symmetry of the lattice, it is natural to compare with the mechanisms and consequences of stripe formation, which has been extensively discussed in the context of cuprate superconductors.⁴⁰ Static stripes also break the translation invariance in addition to the orientational symmetry, and their formation requires interactions with large momentum transfers, such as antiferromagnetic interactions. Many experimental observations, which have been attributed to static or fluctuating stripes,⁴¹ actually provide evidence only for a tendency to orientational, not translational, symmetry-breaking, and could therefore be described equally well by a (incipient) Pomeranchuk instability.

Strong Fermi surface fluctuations could be at least partially responsible for the non-Fermi liquid behavior observed in the ”strange metal” regime of cuprate superconductors near optimal doping. In our model calculation we have obtained a strongly anisotropic anomalously large decay rate for single-particle excitations and a flattening of the dispersion relation near the Fermi surface away from the nodal direction. The properties of single-particle excitations in various cuprate compounds have been investigated in considerable detail by numerous angular resolved photoemission experiments.⁴² Extended flat bands in the van Hove region have been observed by various groups already in the early 1990s.^{43,44,45} Large anisotropic decay rates have been extracted from the linewidth

of low-energy peaks in the photoemission spectra observed in optimally doped cuprates, using in particular momentum scans perpendicular to the Fermi surface at various fixed energies.^{46,47} The line shape of these scans is almost Lorentzian, which is consistent with our results. However, the frequency and temperature dependence of the self-energy extracted from the experimental raw-data differs from what we obtained from d-wave Fermi surface fluctuations. On the other hand, the functional form of the self-energy chosen by the experimentalists may not be the only way to achieve consistency with the photoemission data. In spite of the impressive progress in this experimental technique, the accuracy of such subtle properties as the energy and temperature dependence of the electron self-energy is still limited by resolution and background problems.

Concerning transport, an anisotropic scattering rate with nodes on the Brillouin zone diagonal can very naturally account for the pronounced anisotropy between the intra- and inter-plane mobility of charge carriers, as pointed out by Ioffe and Millis⁴⁸ in their phenomenological "cold spot" scenario. According to their idea, the intra-plane transport is dominated by quasi-particles with a long life-time near the diagonal of the Brillouin zone, while these carriers are not available for inter-plane transport, since transverse hopping amplitudes vanish on the diagonal.

A spin dependent Pomeranchuk instability was recently invoked to explain a new phase observed in ultrapure crystals of the layered ruthenate metal $\text{Sr}_3\text{Ru}_2\text{O}_7$,⁴⁹ and also to account for a puzzling phase transition in URu_2Si_2 .⁵⁰ For a broader comparison with experimental data for cuprate superconductors and other layered materials, which might undergo or be close to a symmetry-breaking Fermi surface deformation, it will be useful to compute experimentally accessible response functions in the presence of strong Fermi surface fluctuations.

Acknowledgments

We thank S. Andergassen, A. Chubukov, C. Di Castro, D. Rohe, M. Vojta, H. Yamase, and especially C. Castellani and A. Katanin for very valuable discussions.

APPENDIX A: BARE POLARIZATION FUNCTION

In this appendix we derive the asymptotic expressions for the bare polarization function $\Pi_d^0(\mathbf{q}, \nu)$ defined in Eq. (7) for small \mathbf{q} and ν . The derivation is valid for arbitrary form factors $d_{\mathbf{p}}$ with any symmetry (not only d-wave), in particular also for the special case $d_{\mathbf{p}} = 1$, for which Π_d^0 reduces to the conventional polarization function Π^0 .

At zero frequency, Π_d^0 can be written as

$$\Pi_d^0(\mathbf{q}, 0) = \int \frac{d^2p}{(2\pi)^2} \frac{f(\xi_{\mathbf{p}+\mathbf{q}/2}) - f(\xi_{\mathbf{p}-\mathbf{q}/2})}{\epsilon_{\mathbf{p}+\mathbf{q}/2} - \epsilon_{\mathbf{p}-\mathbf{q}/2}} d_{\mathbf{p}}^2. \quad (\text{A1})$$

with $\xi_{\mathbf{p}} = \epsilon_{\mathbf{p}} - \mu$. The numerator and the denominator of the fraction under the above integral are odd functions of \mathbf{q} , and the integrand is thus an even function. The denominator can be expanded as

$$\epsilon_{\mathbf{p}+\mathbf{q}/2} - \epsilon_{\mathbf{p}-\mathbf{q}/2} = \mathbf{q} \cdot \mathbf{v}_{\mathbf{p}} + \frac{1}{24} \sum_{j_1, j_2, j_3} \frac{\partial^3 \epsilon_{\mathbf{p}}}{\partial p_{j_1} \partial p_{j_2} \partial p_{j_3}} q_{j_1} q_{j_2} q_{j_3} + \mathcal{O}(|\mathbf{q}|^5) \quad (\text{A2})$$

with $\mathbf{v}_{\mathbf{p}} = \nabla_{\mathbf{p}} \epsilon_{\mathbf{p}}$ and j_1, j_2, j_3 each running over the two possible directions x and y (in two dimensions). The numerator is expanded as

$$f(\xi_{\mathbf{p}+\mathbf{q}/2}) - f(\xi_{\mathbf{p}-\mathbf{q}/2}) = \mathbf{q} \cdot \nabla_{\mathbf{p}} f(\xi_{\mathbf{p}}) + \frac{1}{24} \sum_{j_1, j_2, j_3} \frac{\partial^3 f(\xi_{\mathbf{p}})}{\partial p_{j_1} \partial p_{j_2} \partial p_{j_3}} q_{j_1} q_{j_2} q_{j_3} + \mathcal{O}(|\mathbf{q}|^5). \quad (\text{A3})$$

Using $\nabla_{\mathbf{p}} f(\xi_{\mathbf{p}}) = f'(\xi_{\mathbf{p}}) \mathbf{v}_{\mathbf{p}}$ and

$$\begin{aligned} \sum_{j_1, j_2, j_3} \frac{\partial^3 f(\xi_{\mathbf{p}})}{\partial p_{j_1} \partial p_{j_2} \partial p_{j_3}} q_{j_1} q_{j_2} q_{j_3} &= f'''(\xi_{\mathbf{p}}) (\mathbf{q} \cdot \mathbf{v}_{\mathbf{p}})^3 + 3f''(\xi_{\mathbf{p}}) (\mathbf{q} \cdot \mathbf{v}_{\mathbf{p}}) \sum_{j_1, j_2} \frac{\partial^2 \epsilon_{\mathbf{p}}}{\partial p_{j_1} \partial p_{j_2}} q_{j_1} q_{j_2} \\ &+ f'(\xi_{\mathbf{p}}) \sum_{j_1, j_2, j_3} \frac{\partial^3 \epsilon_{\mathbf{p}}}{\partial p_{j_1} \partial p_{j_2} \partial p_{j_3}} q_{j_1} q_{j_2} q_{j_3} \end{aligned} \quad (\text{A4})$$

one obtains

$$\frac{f(\xi_{\mathbf{p}+\mathbf{q}/2}) - f(\xi_{\mathbf{p}-\mathbf{q}/2})}{\epsilon_{\mathbf{p}+\mathbf{q}/2} - \epsilon_{\mathbf{p}-\mathbf{q}/2}} = f'(\xi_{\mathbf{p}}) + \frac{1}{8} f''(\xi_{\mathbf{p}}) \sum_{j_1, j_2} \frac{\partial^2 \epsilon_{\mathbf{p}}}{\partial p_{j_1} \partial p_{j_2}} q_{j_1} q_{j_2} + \frac{1}{24} f'''(\xi_{\mathbf{p}}) (\mathbf{q} \cdot \mathbf{v}_{\mathbf{p}})^2 + \mathcal{O}(|\mathbf{q}|^4) \quad (\text{A5})$$

Note that terms involving third order derivatives of $\epsilon_{\mathbf{p}}$ have cancelled. Inserting this expansion in Eq. (A1) and using the point group symmetries of the square lattice one obtains

$$\Pi_d^0(\mathbf{q}, 0) = \int \frac{d^2p}{(2\pi)^2} \left[f'(\xi_{\mathbf{p}}) + \frac{1}{16} f''(\xi_{\mathbf{p}}) \Delta \epsilon_{\mathbf{p}} |\mathbf{q}|^2 + \frac{1}{48} f'''(\xi_{\mathbf{p}}) v_{\mathbf{p}}^2 |\mathbf{q}|^2 \right] d_{\mathbf{p}}^2 + \mathcal{O}(|\mathbf{q}|^4), \quad (\text{A6})$$

which establishes Eq. (12) and the formulae for the expansion coefficients $a(T)$ and $c(T)$ presented in Sec. III. In the special case $d_{\mathbf{k}} = 1$ the term involving f'' in the above equation can be rewritten in the form of the term proportional to f''' by a partial integration, yielding the simplified formula for the conventional polarization function

$$\Pi^0(\mathbf{q}, 0) = \int \frac{d^2p}{(2\pi)^2} \left[f'(\xi_{\mathbf{p}}) - \frac{1}{24} f'''(\xi_{\mathbf{p}}) v_{\mathbf{p}}^2 |\mathbf{q}|^2 \right] + \mathcal{O}(|\mathbf{q}|^4). \quad (\text{A7})$$

We now derive the frequency and momentum dependence of $\Pi_d^0(\mathbf{q}, \nu)$ for small \mathbf{q} and ν to leading order in \mathbf{q} and ν . In the limit $\mathbf{q} \rightarrow 0$, $\nu \rightarrow 0$ the polarization function depends only via the ratio $s = \nu/|\mathbf{q}|$ and the unit vector $\hat{\mathbf{q}} = \mathbf{q}/|\mathbf{q}|$ on \mathbf{q} and ν :

$$\Pi_d^0(\mathbf{q}, \nu) \rightarrow - \int \frac{d^2 p}{(2\pi)^2} f'(\xi_{\mathbf{p}}) \frac{\mathbf{v}_{\mathbf{p}} \cdot \hat{\mathbf{q}}}{s + i0^+ - \mathbf{v}_{\mathbf{p}} \cdot \hat{\mathbf{q}}} d_{\mathbf{p}}^2. \quad (\text{A8})$$

In the low temperature limit only momenta on the Fermi surface contribute to the above integral, since then $f'(\xi_{\mathbf{p}}) \rightarrow -\delta(\xi_{\mathbf{p}})$. The real part is an even function of s which tends to $a(T)$ in the limit $s \rightarrow 0$, with corrections of order s^2 . The imaginary part has the simple form

$$\text{Im}\Pi_d^0(\mathbf{q}, \nu) \rightarrow \int \frac{d^2 p}{4\pi} f'(\xi_{\mathbf{p}}) d_{\mathbf{p}}^2 s \delta(s - \mathbf{v}_{\mathbf{p}} \cdot \hat{\mathbf{q}}). \quad (\text{A9})$$

For $\mathbf{q}, \nu \rightarrow 0$ and small s this simplifies further to $\text{Im}\Pi_d^0(\mathbf{q}, \nu) \rightarrow -\rho(\hat{\mathbf{q}}, T) s$ with

$$\rho(\hat{\mathbf{q}}, T) = - \int \frac{d^2 p}{4\pi} f'(\xi_{\mathbf{p}}) d_{\mathbf{p}}^2 \delta(\mathbf{v}_{\mathbf{p}} \cdot \hat{\mathbf{q}}). \quad (\text{A10})$$

At $T = 0$ the integrand in Eq. (A9) contains two δ -functions. The two-dimensional momentum integral can then be carried out, yielding

$$\text{Im}\Pi_d^0(\mathbf{q}, \nu) \rightarrow -\frac{s}{4\pi} \sum_{\mathbf{k}_F^0} d_{\mathbf{k}_F^0}^2 \frac{1}{v_{\mathbf{k}_F^0}} \frac{1}{|\mathbf{t}_{\mathbf{k}_F^0} \cdot \nabla_{\mathbf{k}_F^0}(\hat{\mathbf{q}} \cdot \mathbf{v}_{\mathbf{k}_F^0})|}, \quad (\text{A11})$$

where $\mathbf{t}_{\mathbf{k}_F^0}$ is a unit vector tangential to the Fermi surface in \mathbf{k}_F^0 , and the sum runs over momenta on the Fermi surface which satisfy the equation $\mathbf{v}_{\mathbf{k}_F^0} \cdot \hat{\mathbf{q}} = s$. The formula (18) for $\rho(\hat{\mathbf{q}}, T)$ at $T = 0$ follows directly.

- ¹ I.J. Pomeranchuk, Sov. Phys. JETP **8**, 361 (1958).
- ² H. Yamase and H. Kohno, J. Phys. Soc. Jpn. **69**, 332 (2000); **69**, 2151 (2000).
- ³ C.J. Halboth and W. Metzner, Phys. Rev. Lett. **85**, 5162 (2000).
- ⁴ I. Grote, E. Körding, and F. Wegner, J. Low Temp. Phys. **126**, 1385 (2002); V. Hankevych, I. Grote, and F. Wegner, Phys. Rev. B **66**, 094516 (2002).
- ⁵ B. Valenzuela and M.A.H. Vozmediano, Phys. Rev. B **63** 153103 (2001).
- ⁶ V. Oganesyan, S.A. Kivelson, and E. Fradkin, Phys. Rev. B **64**, 195109 (2001).
- ⁷ S.A. Kivelson, E. Fradkin, and V.J. Emery, Nature **393**, 550 (1998).
- ⁸ A. Neumayr and W. Metzner, Phys. Rev. B **67**, 035112 (2003).
- ⁹ M. Vojta, Y. Zhang, and S. Sachdev, Phys. Rev. Lett. **85**, 4940 (2000); Int. J. Mod. Phys. B **14**, 3719 (2000).
- ¹⁰ W. Metzner, D. Rohe, and S. Andergassen, Phys. Rev. Lett. **91**, 066402 (2003).

- ¹¹ H.-Y. Kee, E.H. Kim, and C.-H. Chung, Phys. Rev. B **68**, 245109 (2003).
- ¹² I. Khavkine, C.-H. Chung, V. Oganesyan, and H.-Y. Kee, Phys. Rev. B **70**, 155110 (2004).
- ¹³ H. Yamase, V. Oganesyan, and W. Metzner, Phys. Rev. B **72**, 035114 (2005).
- ¹⁴ P.A. Frigeri, C. Honerkamp, and T.M. Rice, Eur. Phys. J. B **28**, 61 (2002).
- ¹⁵ This correlation function has been recently analyzed within slave boson RPA for the t-J model, see H. Yamase, Phys. Rev. Lett. **93**, 266404 (2004).
- ¹⁶ T. Moriya, *Spin Fluctuations in Itinerant Electron Magnetism* (Springer, Berlin, 1985).
- ¹⁷ The velocity $u(\hat{\mathbf{q}})$ shouldn't be confused with the interaction $u(\mathbf{q})$ introduced in Sec. II.
- ¹⁸ A.V. Chubukov and D.L. Maslov, Phys. Rev. B **68**, 155113 (2003), and references therein.
- ¹⁹ A. Chubukov, private communication.
- ²⁰ J. Zinn-Justin, *Quantum Field Theory and Critical Phenomena* (Oxford University Press, New York, 1996).
- ²¹ J.A. Hertz, Phys. Rev. B **14**, 1165 (1976).
- ²² A.J. Millis, Phys. Rev. B **48**, 7183 (1993).
- ²³ C. Castellani, C. Di Castro, and M. Grilli, Phys. Rev. Lett. **75**, 4650 (1995).
- ²⁴ A. Chubukov, Phys. Rev. B **71**, 245123 (2005).
- ²⁵ P.A. Lee, Phys. Rev. Lett. **63**, 680 (1989).
- ²⁶ B. Blok and H. Monien, Phys. Rev. B **47**, 3454 (1993).
- ²⁷ Ar. Abanov, A.V. Chubukov, and J. Schmalian, Adv. Phys. **52**, 119 (2003).
- ²⁸ B.L. Altshuler, L.B. Ioffe, and A.J. Millis, Phys. Rev. B **50**, 14048 (1994).
- ²⁹ Y.M. Vilk and A.-M.S. Tremblay, J. Phys. I (France) **7**, 1309 (1997).
- ³⁰ A.A. Katanin, A.P. Kampf, and V.Yu. Irkhin, Phys. Rev. B **71**, 085105 (2005); A.A. Katanin, Phys. Rev. B **72**, 035111 (2005).
- ³¹ A.A. Katanin, private communication.
- ³² C. Castellani, S. Caprara, C. Di Castro, and A. Maccarone, Nucl. Phys. B **594**, 747 (2001).
- ³³ J.D. Axe, A.H. Moudden, D. Hohlwein, D.E. Cox, K.M. Mohanty, A.R. Moodenbaugh, and Youwen Xu, Phys. Rev. Lett. **62**, 2751 (1989).
- ³⁴ B. Büchner, M. Breuer, A. Freimuth, and A.P. Kampf, Phys. Rev. Lett. **73**, 1841 (1994).
- ³⁵ H. Yamase and H. Kohno, J. Phys. Soc. Jpn. **70**, 2733 (2001); *ibid* **71**, 1154 (2002).
- ³⁶ D.H. Lu, D.L. Feng, N.P. Armitage, K.M. Shen, A. Damascelli, C. Kim, F. Ronning, Z.-X. Shen, D.A. Bonn, R. Liang, W.N. Hardy, A.I. Rykov, and S. Tajima Phys. Rev. Lett. **86**, 4370 (2001).
- ³⁷ Y. Ando, K. Segawa, S. Komiya, and A.N. Lavrov, Phys. Rev. Lett. **88**, 137005 (2002).
- ³⁸ V. Hinkov, S. Pailhes, P. Bourges, Y. Sidis, A. Ivanov, A. Kulakov, C.T. Lin, D.P. Chen, C. Bernhard, and B. Keimer, Nature **430**, 650 (2004).
- ³⁹ O.K. Andersen, A.I. Liechtenstein, O. Jepsen, and F. Paulsen, J. Phys. Chem. Solids **56**, 1573 (1995).
- ⁴⁰ See, for example, Proc. of 3rd Int. Conf. on *Stripes and High T_c superconductivity*, Int. J.

- Mod. Phys. B **14**, Nos. 29-31 (2000).
- ⁴¹ S.A. Kivelson, I.P. Bindloss, E. Fradkin, V. Oganessian, J.M. Tranquada, A. Kapitulnik, and C. Howald, Rev. Mod. Phys. **75**, 1201 (2003).
- ⁴² For a recent review on photoemission in cuprates, see A. Damascelli, Z. Hussain, and Z.X. Shen, Rev. Mod. Phys. **75**, 473 (2003).
- ⁴³ A.A. Abrikosov, J.C. Campuzano, and K. Gofron, Physica C **214**, 73 (1993).
- ⁴⁴ D.S. Dessau, Z.-X. Shen, D.M. King, D.S. Marshall, L.W. Lombardo, P.H. Dickinson, A.G. Loeser, J. DiCarlo, C.-H. Park, A. Kapitulnik, and W.E. Spicer, Phys. Rev. Lett. **71**, 2781 (1993).
- ⁴⁵ K. Gofron, J.C. Campuzano, H. Ding, C. Gu, R. Liu, B. Dabrowski, B.W. Veal, W. Cramer, and G. Jennings, J. Phys. Chem. Solids **54**, 1193 (1993).
- ⁴⁶ T. Valla, A.V. Fedorov, P.D. Johnson, Q. Li, G.D. Gu, and N. Koshizuka, Phys. Rev. Lett. **85**, 828 (2000).
- ⁴⁷ A. Kaminski, H.M. Fretwell, M.R. Norman, M. Randeria, S. Rosenkranz, U. Chatterjee, J.C. Campuzano, J. Mesot, T. Sato, T. Takahashi, T. Terashima, M. Takano, K. Kadowaki, Z.Z. Li, and H. Raffy, Phys. Rev. B **71**, 014517 (2005).
- ⁴⁸ L.B. Ioffe, and A.J. Millis, Phys. Rev. B **58**, 11631 (1998).
- ⁴⁹ S.A. Grigera, P. Gegenwart, R.A. Borzi, F. Weickert, A.J. Schofield, R.S. Perry, T. Tayama, T. Sakakibara, Y. Maeno, A.G. Green, and A.P. Mackenzie, Science **306**, 1154 (2004).
- ⁵⁰ C.M. Varma and L. Zhu, cond-mat/0502344.

$$\Gamma = \overset{\mathbf{f}}{\text{~~~~~}} + \overset{\mathbf{f}}{\text{~~~~~}} \text{ (bubble) } \overset{\mathbf{f}}{\text{~~~~~}} + \dots$$

FIG. 1: Series of bubble chains contributing to the effective interaction Γ .

$$\Sigma = \text{~~~~~} \overset{\Gamma}{\text{~~~~~}} \text{~~~~~}$$

FIG. 2: Fock diagram relating the self-energy Σ to the effective interaction Γ .

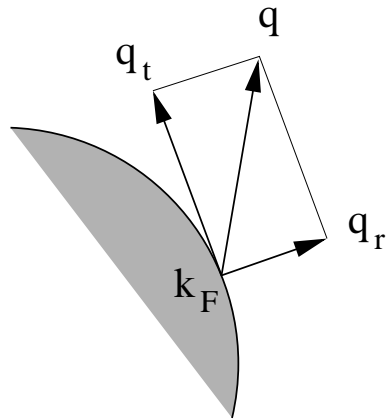


FIG. 3: Decomposition of momentum transfers \mathbf{q} in normal and tangential components relative to the Fermi surface in \mathbf{k}_F .

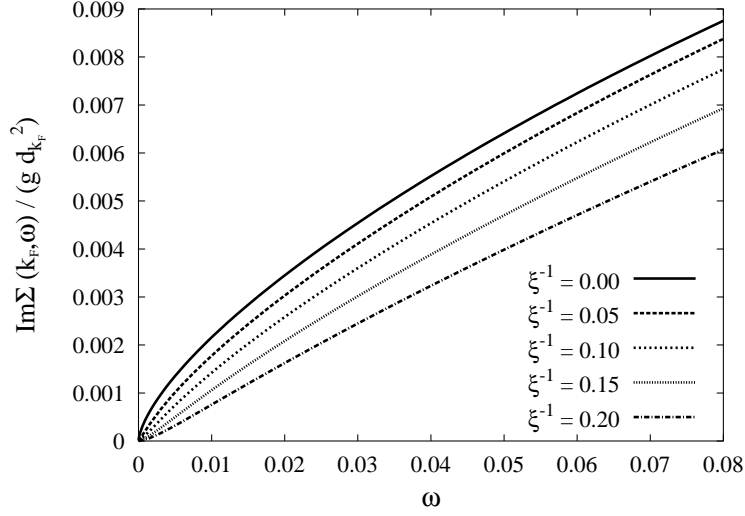


FIG. 4: Non-selfconsistent RPA result for the imaginary part of the self-energy $\text{Im}\Sigma(\mathbf{k}_F, \omega)$, divided by $gd_{\mathbf{k}_F}^2$, as a function of ω in the ground state ($T = 0$) for various choices of the correlation length ξ ; the other relevant parameters are $\xi_0 = v_{\mathbf{k}_F} = u_{\mathbf{k}_F} = 1$.

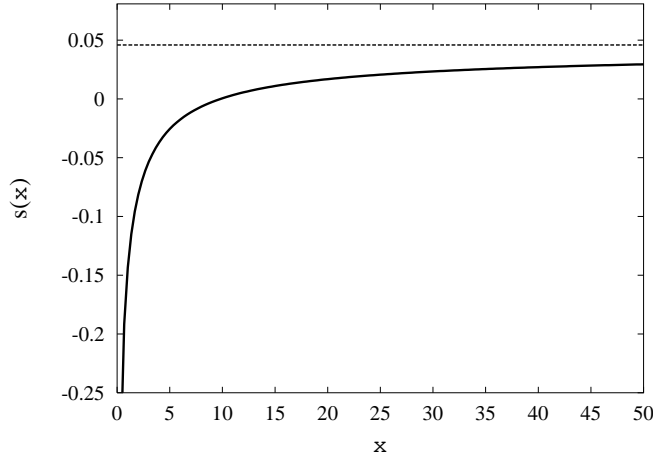


FIG. 5: Scaling function $s(x)$ describing the asymptotic behavior of the quantum contribution to $\text{Im}\Sigma(\mathbf{k}_F, \omega)$ at low ω and T ; the horizontal line indicates the asymptotic value of $s(x)$ for large x .

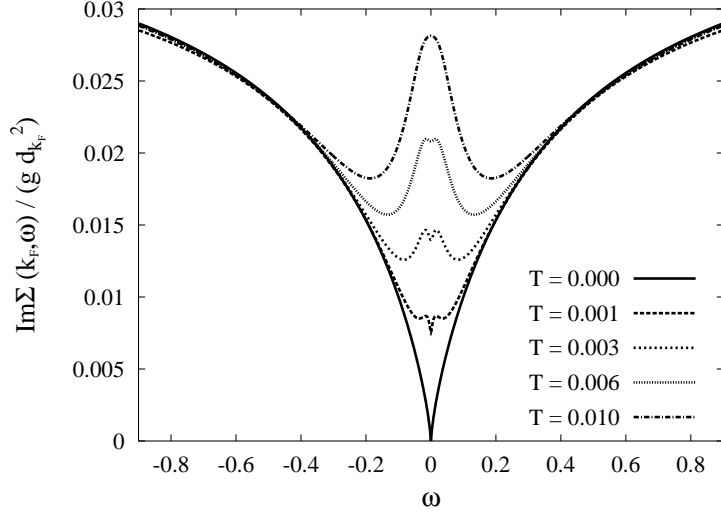


FIG. 6: Non-selfconsistent RPA result for the imaginary part of the self-energy $\text{Im}\Sigma(\mathbf{k}_F, \omega)$, divided by $g d_{\mathbf{k}_F}^2$, as a function of ω for several temperatures T with a correlation length $\xi(T) = 3/|T \log T|^{1/2}$; the other relevant parameters are $\xi_0 = v_{\mathbf{k}_F} = u = 1$.

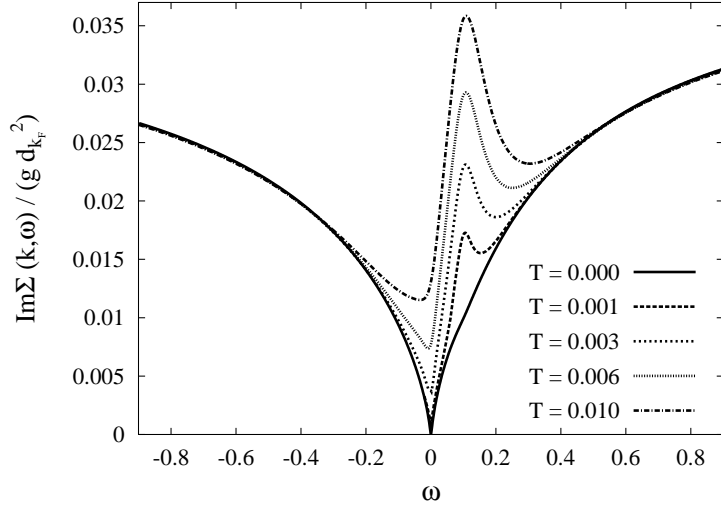


FIG. 7: Non-selfconsistent RPA result for $\text{Im}\Sigma(\mathbf{k}, \omega)$ as in Fig. 6, but now for $k_r = 0.1$, that is $\mathbf{k} \neq \mathbf{k}_F$.

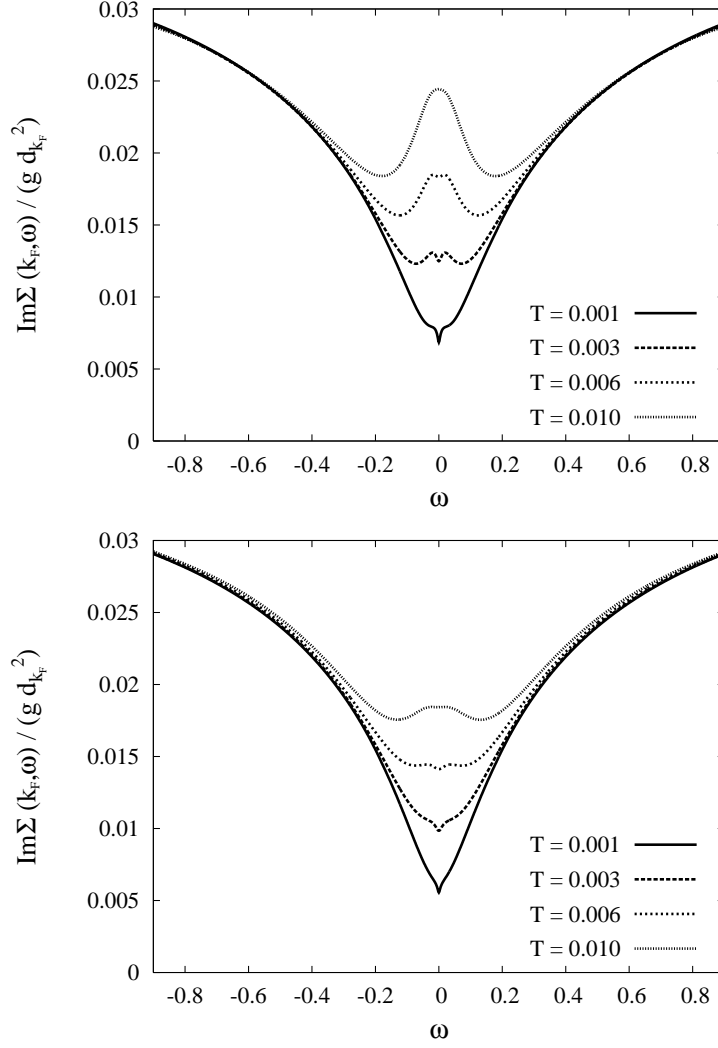


FIG. 8: Selfconsistent RPA results for the imaginary part of the self-energy $\text{Im}\Sigma(\mathbf{k}_F, \omega)$, divided by $g d_{\mathbf{k}_F}^2$, as a function of ω for several temperatures T , with a correlation length $\xi(T) = 3/|T \log T|^{1/2}$ and $\xi_0 = v_{\mathbf{k}_F} = u = 1$. Upper panel: $|g|d_{\mathbf{k}_F}^2 = 1$, lower panel: $|g|d_{\mathbf{k}_F}^2 = 4$.

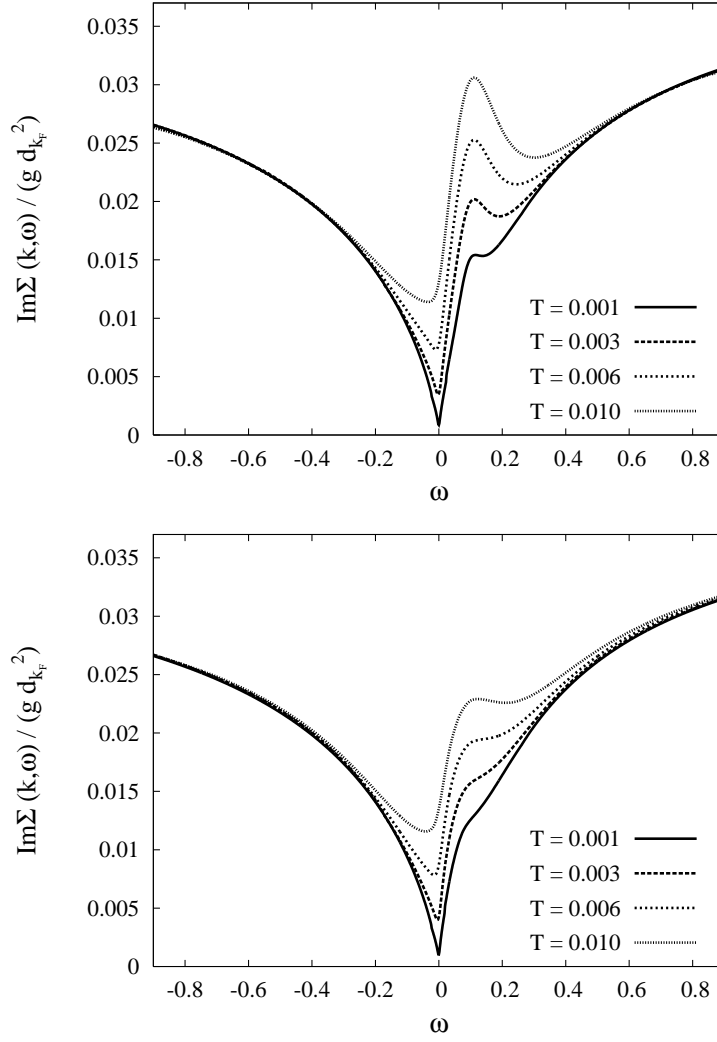


FIG. 9: Self-consistent RPA result for $\text{Im}\Sigma(\mathbf{k}, \omega)$ as in Fig. 8, but now for $k_r = 0.1$.

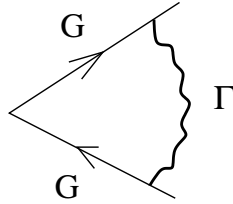


FIG. 10: Feynman diagram representing the first order vertex correction.

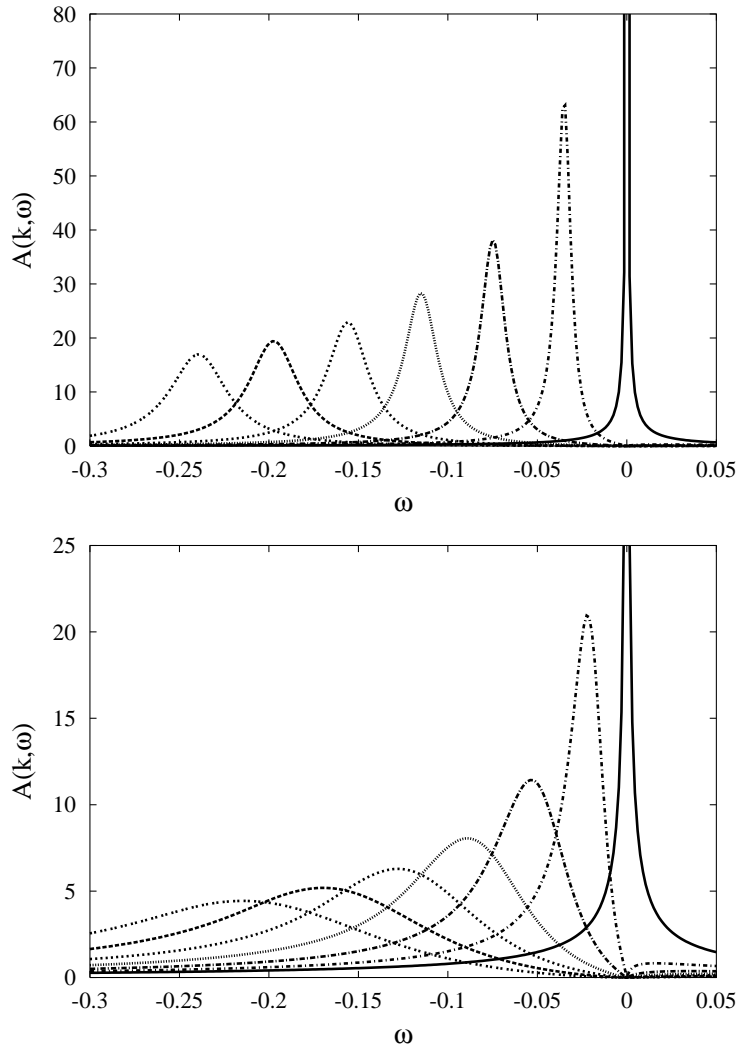


FIG. 11: Spectral function $A(\mathbf{k}, \omega)$ at the quantum critical point as a function of ω for $k_r = -0.0405n$ with $n = 0, 1, 2, \dots, 6$. Fixed parameters are $\xi_0 = v_{\mathbf{k}_F} = u = 1$. Upper panel: $|g|d_{\mathbf{k}_F}^2 = 1$, lower panel: $|g|d_{\mathbf{k}_F}^2 = 4$.

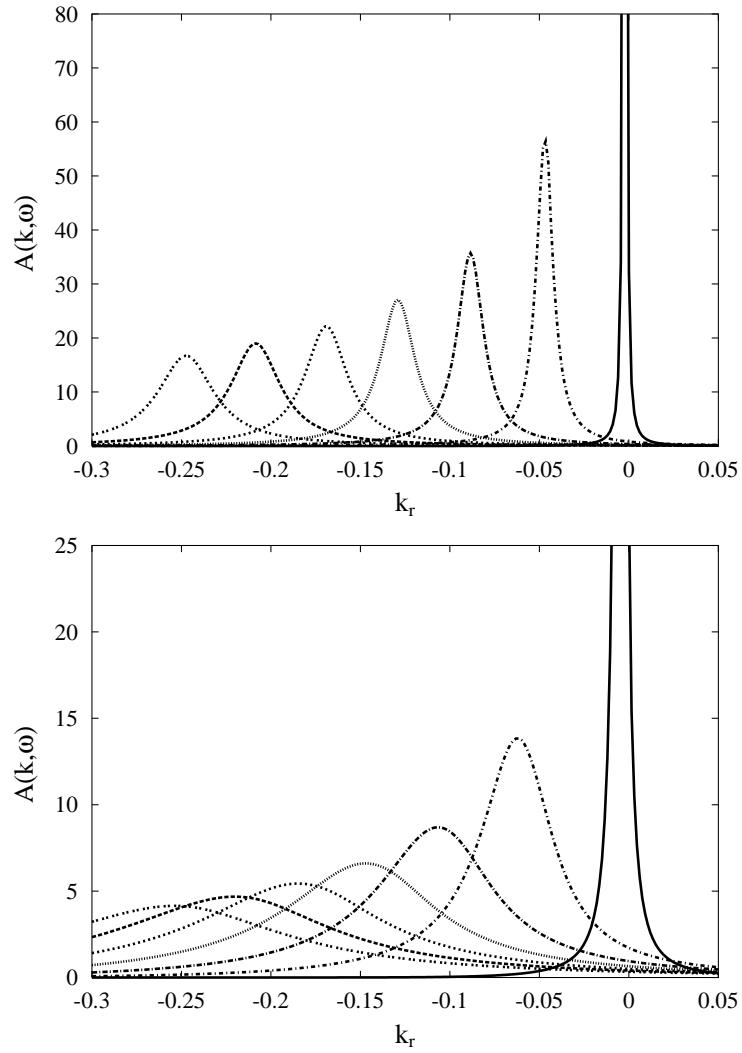


FIG. 12: Momentum scans of $A(\mathbf{k}, \omega)$ at the quantum critical point for $\omega = -0.0015 - 0.0405 n$ with $n = 0, 1, 2, \dots, 6$. The parameters are the same as in Fig. 11.

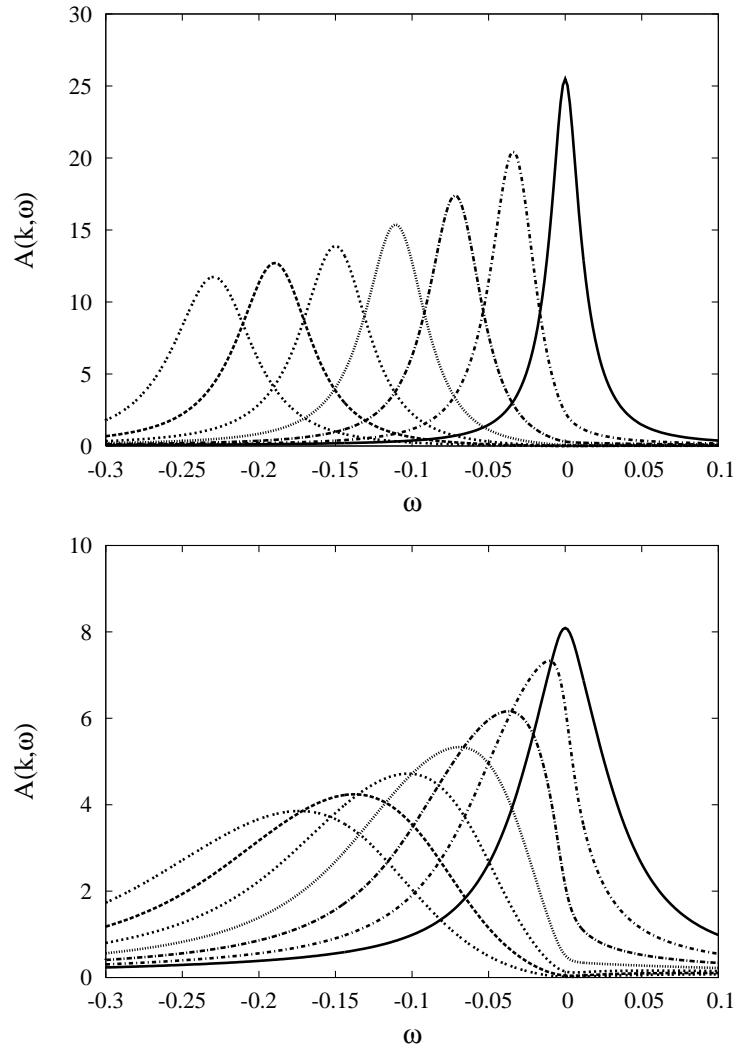


FIG. 13: Spectral function $A(\mathbf{k}, \omega)$ at $T = 0.003$ as a function of ω for $k_r = -0.0405n$ with $n = 0, 1, 2, \dots, 6$. Parameters and $\xi(T)$ as in Fig. 8.

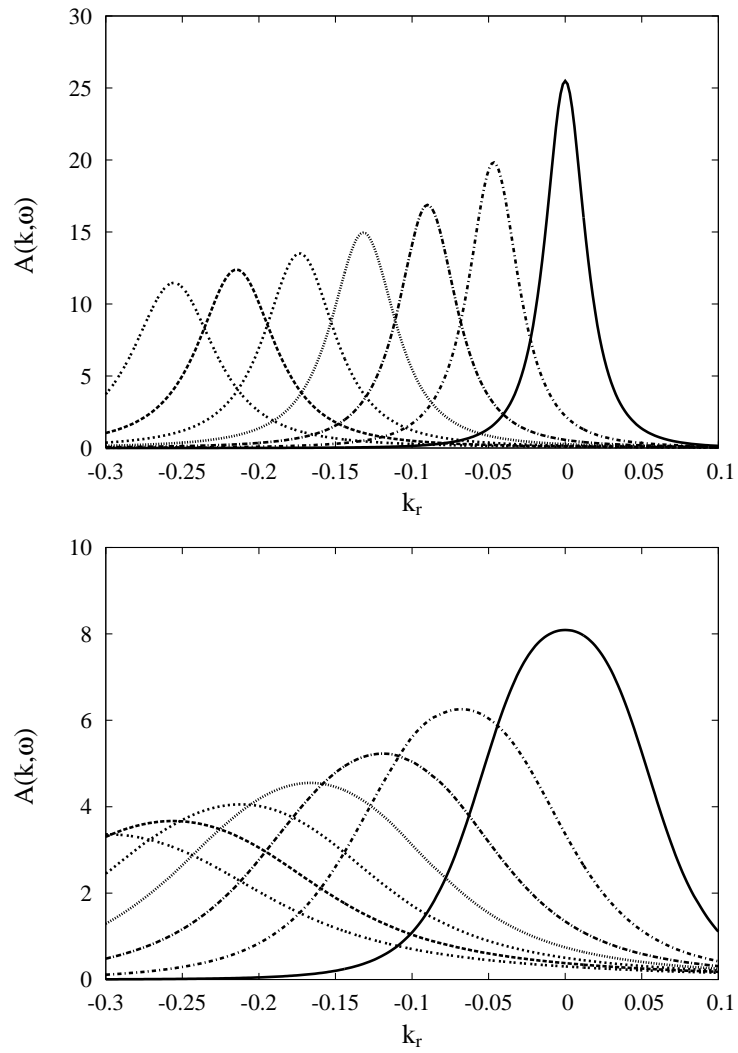


FIG. 14: Momentum scans of $A(\mathbf{k}, \omega)$ at $T = 0.003$ for $\omega = -0.0405 n$ with $n = 0, 1, 2, \dots, 6$. Parameters and $\xi(T)$ as in Fig. 8.